GEOLOGICA CARPATHICA, FEBRUARY 2022, 73, 1, 3–23 https://doi.org/10.31577/GeolCarp.73.1.1

Low-temperature constraints on the Alpine thermal evolution of the central parts of the Sredna Gora Zone, Bulgaria

ELEONORA BALKANSKA[1,✉], STOYAN GEORGIEV[2], ALEXANDRE KOUNOV[3], MILORAD ANTIĆ[4], TAKAHIRO TAGAMI[5], SHIGERU SUEOKA[6], JAN WIJBRANS[7] and IRENA PEYTCHEVA[2]

[1]Department of Geology, Paleontology and Fossil Fuels, Sofia University, 1504 Sofia, Bulgaria; ✉balkanska@gea.uni-sofia.bg
[2]Geological Institute, Bulgarian Academy of Sciences, Sofia, Bulgaria; kantega@abv.bg, peytcheva@erdw.ethz.ch
[3]Department of Environmental Sciences, Basel University, 4056 Basel, Switzerland; a.kounov@unibas.ch
[4]Zlatna Reka Resources, Belgrade, Serbia; m.antic@zlatnareka.com
[5]Department of Geology and Mineralogy, Kyoto University, 606-8502 Kyoto, Japan; tagami@kueps.kyoto-u.ac.jp
[6]Tono Geoscience Center, Japan Atomic Energy Agency, 509-5102 Toki, Japan; sueoka.shigeru@jaea.go.jp
[7]Department of Earth Sciences, Vrije Universiteit Amsterdam, 1081 HV Amsterdam, the Netherlands; j.r.wijbrans@vu.nl

(Manuscript received July 11, 2021; accepted in revised form January 20, 2022; Associate Editor: Milan Kohút)

Abstract: The central parts of the Sredna Gora Zone in Bulgaria have experienced a complex Alpine tectonic evolution. The main tectonic and thermal events since the end of the Triassic are the Late Jurassic–Early Cretaceous (Early Alpine) and Late Cretaceous–Paleogene (Late Alpine) compression separated by Late Cretaceous volcanic-arc magmatism and intra/back-arc extension and basin formation. During most of the Cenozoic, the area was mainly under post-orogenic extension. Here, we present the first apatite and zircon fission-track results and new muscovite and biotite $^{40}Ar/^{39}Ar$ analysis on upper Carboniferous–Permian granitoids together with Upper Cretaceous volcanic and subvolcanic rocks and Upper Maastrichtian–Danian conglomerates from the Panagyurishte basin, which allowed us to reveal the Alpine thermal and tectonic evolution of the central parts of the Sredna Gora Zone. Our new results disclosed the existence of several thermal and cooling episodes related to different tectonic and magmatic events in the studied area. The $^{40}Ar/^{39}Ar$ dating of samples from the metamorphic basement constrain the thermal peak of an Early Alpine thermal event at about 140–138 Ma at temperatures between ~300 and 400 °C. Through the apatite FT dating and thermal modelling, the time of a Late Alpine (post-Danian) event was constrained at 65–55 Ma, during which the tectonically buried sediments of the Panagyurishte basin reached temperatures of <120 °C. The post-early Eocene cooling and exhumation of the central parts of the Sredna Gora Zone metamorphic basement was related to post-orogenic extension and denudation which took place probably in two stages during the middle Eocene to Oligocene.

Keywords: Bulgaria, central parts of the Sredna Gora Zone, LA–ICP–MS fission-track dating, $^{40}Ar/^{39}Ar$ multiple single-grain fusion dating, thermal evolution.

Introduction

The Sredna Gora Zone in Bulgaria, confined between the Balkan fold-thrust belt to the north and the Rhodope metamorphic complex to the south, is a part of the Balkan orogenic system (Fig. 1, Ivanov 1983, 2017). The latter was formed during two major compressional phases of the Alpine (post-Triassic) orogeny named in the Bulgarian literature as Early Alpine (Late Jurassic–Early Cretaceous) and Late Alpine (Late Cretaceous–Paleogene), respectively (e.g. Ivanov 2017). During Alpine time the Sredna Gora Zone was a part of the hinterland of the Balkan fold-thrust belt involved in north-vergent thrusting (e.g. Bončev 1940; Vangelov et al. 2013; Burchfiel & Nakov 2015). The compressional phases were separated by a Late Cretaceous extensional event, during which a magmatic arc and an intra-arc/back-arc basin system formed, part of the large peri-Tethyan magmatic belt (e.g. Aiello et al. 1977; Boccaletti et al. 1978; von Quadt et al. 2005; Gallhofer et al. 2015).

Logically the evolution of the magmatic arc, related to the formation of important copper and polymetallic ore deposits, attracted much more attention of the scientists than the rest of the geological history of the Sredna Gora Zone (e.g. Strashimirov et al. 2002; von Quadt et al. 2005; Kamenov et al. 2007; Gallhofer et al. 2015). The structural studies dedicated to the Early Alpine tectonics of the central parts of the Sredna Gora Zone are limited, probably due to scarce lower Mesozoic cover preserved in the zone (Zagorchev et al. 2009; Lazarova et al. 2015; Ivanov 2017). Additionally, it is challenging to recognize the structures related to this phase in the basement rocks and distinguish them from those formed during its pre-Permian evolution due to the fact that they all represent low-grade discrete shear zones. On the other hand, more attention was devoted to the Early Alpine structures along the contact between the Sredna Gora Zone and the Balkan fold-thrust belt (e.g. Gerdjikov & Georgiev 2005, 2006; Gerdjikov et al. 2007). Several tectonic studies are dedicated to the Late Alpine phase, which was relatively better recorded in the partly preserved Upper Cretaceous sediments

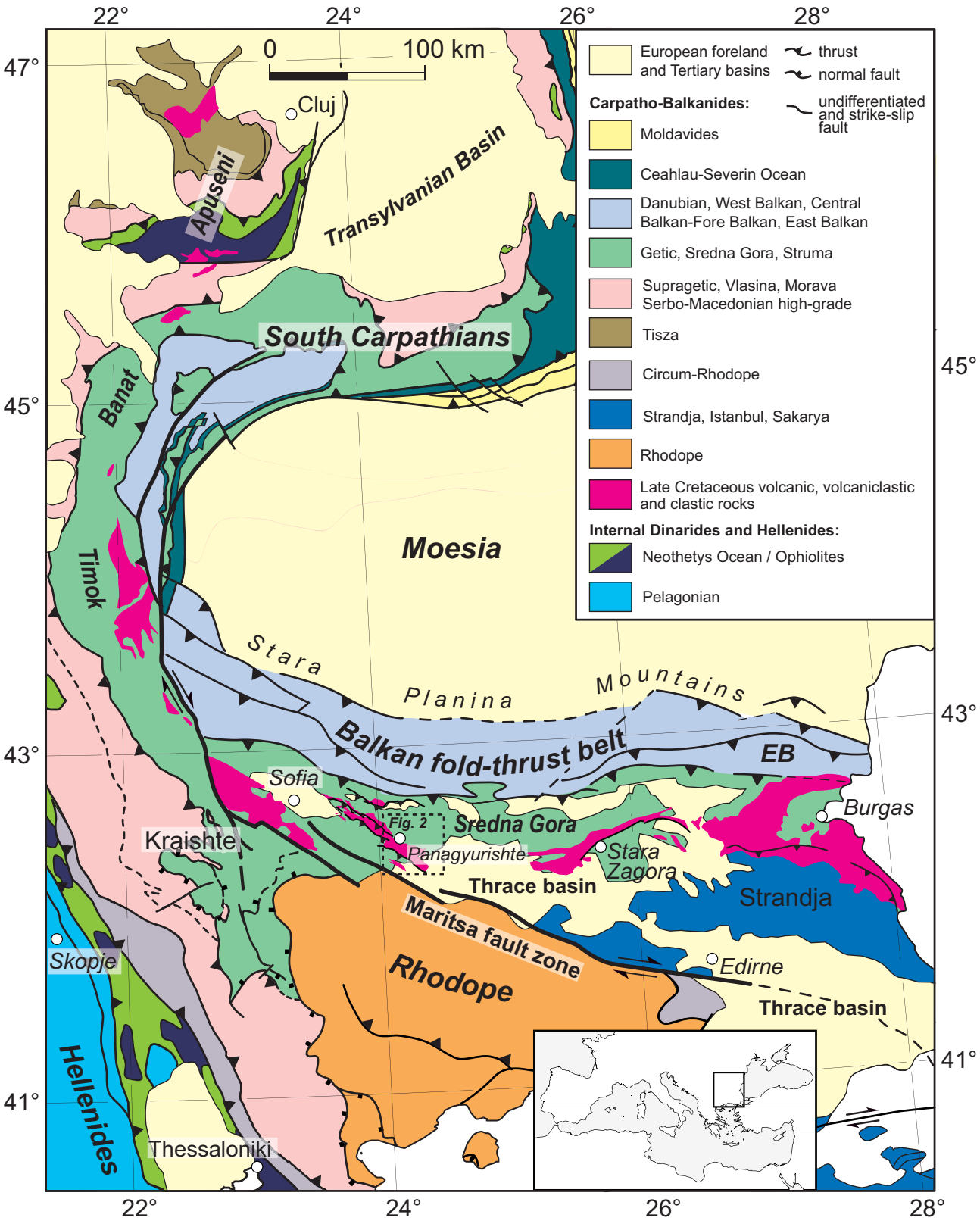

Fig. 1. Tectonic map of the central part of the Balkan Peninsula (modified after Schmid et al. 2008) showing the major tectonic units. EB=East Balkan.

of the intra-arc/back-arc basins (Bončev 1970; Karagjuleva et al. 1972; 1974; Gerdjikov et al. 2019, 2020; Kounov & Gerdjikov 2020). Nevertheless, even this part of the evolution of the area is poorly constrained as geo- and thermochronological studies are scarce (Handler et al. 2004).

Several stages of compression, extension and strike-slip tectonics have affected the Sredna Gora Zone during the Cenozoic (e.g. Burchfiel et al. 2008). Recently, together with the large number of tectonic studies, several thermochronological studies, concerning the evolution of the neighbouring Rhodope and Balkan fold-thrust belt, were presented (Kounov et al. 2015, 2018, 2020; Stübner et al. 2016; Gunnell et al. 2017). However, the Sredna Gora Zone remained outside the scope of this type of investigation. The only studies related to the Cenozoic extension of the central parts of the Sredna Gora Zone are those on the evolution of the Thrace basin, although most of them are dedicated to its south-eastern part, far from our study area (Fig. 1, Cavazza et al. 2013; Caracciolo et al. 2015; Popov et al. 2015). Several studies discussed the Cenozoic evolution of the Maritsa strike-slip shear zone to the south of the study area (Gerdjikov & Georgiev 2006; Naydenov et al. 2013; Gerdjikov et al. 2015), but they are related mostly to the deformation along this shear zone rather than to the tectonic evolution of the Sredna Gora Zone.

In order to unravel the thermal and tectonic evolution of the central parts of the Sredna Gora Zone during Alpine time, we performed low-temperature thermochronological analysis, including $^{40}Ar/^{39}Ar$ dating combined with apatite and zircon fission-track analysis. The LA–ICP–MS fission-track analyses were carried out in the newly established Low-Temperature Thermochronology Laboratory in Bulgaria, whereas the biotite and muscovite multiple single-grain fusion $^{40}Ar/^{39}Ar$ dating was performed at the Vrije Universiteit of Amsterdam. Our target region was the central part of the Sredna Gora Zone, where the Upper Cretaceous sediments of the Panagyurishte basin crop out together with their Variscan crystalline basement (Fig. 2). The obtained results represent the first quantitative estimates of the time and amount of the tectonic burial during the Late Cretaceous–Paleocene event as well as the time and rate of exhumation during the following Eocene–Oligocene extension in the area.

Geological setting

Variscan basement

The Variscan metamorphic basement of the central parts of the Sredna Gora Zone consists of high-grade metamorphic rocks dominated by micaceous paragneiss, hornblende–biotite gneiss, amphibolite and ultramafic bodies, affected by migmatization (Katskov & Iliev 1993; Zagorchev 2008). The protoliths of the orthogneiss are of Ediacaran–late Cambrian age (Peytcheva & von Quadt 2004; Carrigan et al. 2006; Antonov et al. 2010; Lazarova et al. 2015). The metamorphic evolution of the crystalline basement includes an Early Devonian eclogite facies metamorphic event followed shortly by an early amphibolite facies re-equilibration (398±5.2 Ma, Gaggero et al. 2009) and Early Carboniferous HT metamorphism (336.5±5.4 Ma, Carrigan et al. 2006). An intense greenschist to lower amphibolite facies regional-scale retrogression and contemporaneous emplacement of pegmatitic dykes was dated at 333.9±0.2 Ma (Gerdjikov et al. 2010). The retrograde metamorphism was followed by a post-metamorphic cooling between 317 and 305 Ma (Velichkova et al. 2004).

The metamorphic basement of the central parts of the Sredna Gora Zone is intruded by several upper Carboniferous–Permian granitic to granodioritic plutons (Dabovski et al. 1966; Zagorchev et al. 1973), part of a large batholith (Fig. 2). Dabovski et al. (1966) defined three intrusive complexes according to their petrographic characteristics and cross-cutting relationships. The first intrusive complex in the study area, presented by the Smilovene pluton (304.1±5.5 Ma, Carrigan et al. 2005), is dominated by biotite granite to granodiorite with mafic enclaves and small gabbro intrusions. The second intrusive complex is represented by biotite and two-mica granite and rare granodiorite and plagiogranite of the Koprivshtitsa pluton dated at 304.8±0.8 Ma (von Quadt et al. 2004) and at 312.0±5.4 Ma (Carrigan et al. 2005). The younger (third) complex includes several biotite and two-mica leucocratic granites presented in the study area by the Strelcha (289.5±7.8 Ma, Carrigan et al. 2005) and Karavelovo plutons (Fig. 2).

Early Alpine phase

The Early Alpine tectonic event (Late Jurassic–Early Cretaceous) was related to the closure of a Triassic–Early Cretaceous basin (part of the Neo-Tethys ocean, Stampfli & Hochard 2009) and formation of north-vergent regional thrusts (e.g. Vangelov et al. 2013; Burchfiel & Nakov 2015; Ivanov 2017). Evidence for this phase in the studied area could be better observed in the Triassic to Lower Jurassic sediments overlying transgressively the crystalline basement (Katskov & Iliev 1993; Zagorchev & Budurov 2009; Ivanov 2017). However, the structural data related to this tectonic event are limited. The Chuminska shear zone, outcropping within the metamorphic basement north of Koprivshtitsa, was reported as a Late Alpine reverse fault (Dabovski et al. 1966) or a Variscan ductile shear zone (Antonov et al. 2010). Since the shear zone postdates the Variscan high-temperature fabric, and due to the structural similarities (temperature conditions and kinematics) with other Early Alpine shear zones in the Balkan fold-thrust belt (e.g. Gerdjikov et al. 2007; Lazarova & Gerdjikov 2008), Lazarova et al. (2015) assumed an Early Alpine age for the greenschist facies shearing or probable reactivation along this zone. Velichkova et al. (2004) interpreted the muscovite and biotite $^{40}Ar/^{39}Ar$ ages between 105 and 99 Ma, obtained from the high-grade metamorphic rocks, as a result of low-grade metamorphism and ductile deformation related to the same Early Alpine tectonic event.

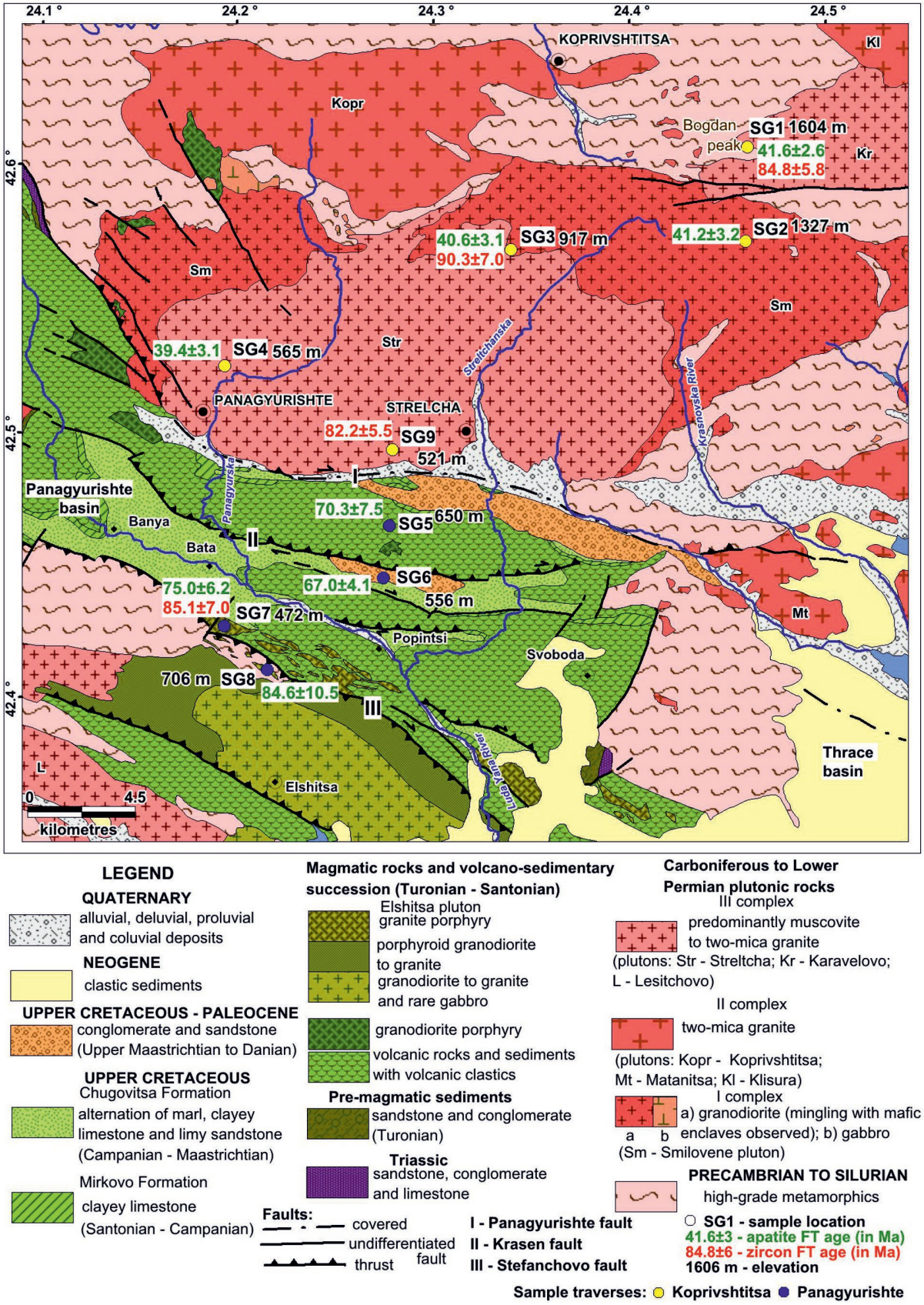

LEGEND

QUATERNARY
alluvial, deluvial, proluvial and coluvial deposits

NEOGENE
clastic sediments

UPPER CRETACEOUS - PALEOCENE
conglomerate and sandstone (Upper Maastrichtian to Danian)

UPPER CRETACEOUS
Chugovitsa Formation
alternation of marl, clayey limestone and limy sandstone (Campanian - Maastrichtian)

Mirkovo Formation
clayey limestone (Santonian - Campanian)

Magmatic rocks and volcano-sedimentary succession (Turonian - Santonian)

Elshitsa pluton
granite porphyry
porphyroid granodiorite to granite
granodiorite to granite and rare gabbro
granodiorite porphyry
volcanic rocks and sediments with volcanic clastics

Pre-magmatic sediments
sandstone and conglomerate (Turonian)

Triassic
sandstone, conglomerate and limestone

Faults:
covered
undifferentiated fault
thrust fault

I - Panagyurishte fault
II - Krasen fault
III - Stefanchovo fault

Carboniferous to Lower Permian plutonic rocks

III complex
predominantly muscovite to two-mica granite
(plutons: Str - Streltcha; Kr - Karavelovo; L - Lesitchovo)

II complex
two-mica granite
(plutons: Kopr - Koprivshtitsa; Mt - Matanitsa; Kl - Klisura)

I complex
a) granodiorite (mingling with mafic enclaves observed); b) gabbro
(Sm - Smilovene pluton)

PRECAMBRIAN TO SILURIAN
high-grade metamorphics

SG1 - sample location
41.6±3 - apatite FT age (in Ma)
84.8±6 - zircon FT age (in Ma)
1606 m - elevation

Sample traverses: Koprivshtitsa Panagyurishte

Fig. 2. Geological map of the studied area with location and FT ages of the analysed samples (modified after Iliev & Kazkov 1990 and Ivanov 2017).

Late Cretaceous magmatic arc

During the Late Cretaceous, the Sredna Gora Zone was part of the Apuseni–Banat–Timok–Sredna Gora magmatic and metallogenic belt formed along the southern European margin, above the Neo-Tethys subducting slab (Fig. 1, e.g. Popov et al. 2002b; von Quadt et al. 2005; Gallhofer et al. 2015). Several arc-related continental basins opened from east to west and were filled with thick Cenomanian to Maastrichtian volcano-sedimentary sequences, associated with abundant magmatism (Fig. 1, Aiello et al. 1977; Boccaletti et al. 1978; Nachev & Nachev 2001; Dabovski et al. 2009; Gallhofer et al. 2015). The Panagyurishte basin (Bončev 1940), located in the central parts of the Sredna Gora Zone (Figs. 1 and 2), is characterized by variable and laterally changing lithological successions of Turonian–Maastrichtian age (e.g. Dimitrova et al. 1984; Vangelov et al. 2019). The contemporaneous calc-alkaline to high-K calc-alkaline volcanism is predominantly of intermediate composition and represented mainly by lava and pyroclastic flows as well as emplacement of several small shallow intrusive bodies (e.g. Boccaletti et al. 1978; Stanisheva-Vassileva 1980; Kamenov et al. 2007; Nedialkov et al. 2007; Peytcheva et al. 2009). Numerous, predominantly porphyry-Cu and Au deposits are related to this magmatic activity (e.g. von Quadt et al. 2005). The timing of the magmatism in the area of the Panagyurishte basin was constrained between 90 and 86 Ma (von Quadt et al. 2005; Peytcheva et al. 2009). The age of the granites of the Elshitsa pluton, located in the south-western part of the study area (Fig. 2) is 86.61±0.31 Ma (U–Pb zircon dating, Peytcheva et al. 2008). The emplacement of the volcanic rocks in the Panagyurishte basin area range between 91 and 84 Ma ($^{40}Ar/^{39}Ar$; Rieser et al. 2008). Handler et al. (2004) reported amphibole and biotite $^{40}Ar/^{39}Ar$ ages from volcanic and subvolcanic rocks between 85 and 80 Ma, also similar to the cited above U–Pb zircon ages of the magmatic rocks in the study area.

The post-magmatic stage of the basin evolution is related to the deposition of epiclastic sediments (mainly Coniacian) followed by the Santonian to Maastrichtian carbonates and clastic deposits of the Mirkovo and Chugovitsa Formations, respectively (Fig. 2, Moev & Antonov 1978; Dimitrova et al. 1984; Vangelov et al. 2019). Based on U–Pb zircon and $^{40}Ar/^{39}Ar$ data from plutonic and volcanic rocks, coupled with the orientation of dyke swarms, Handler et al. (2004) and Rieser et al (2008) distinguished two main stages in the Late Cretaceous basin and magmatic evolution. The first stage, constrained between 93 and 89 Ma, was related to N–S back-arc extension driven by slab roll-back (e.g. Kamenov et al. 2007). The second stage, between 86 and 78 Ma, was associated with N–S compression combined with dextral shearing caused by the arrival of a hypothetical microcontinent in the trench zone, which induced horizontal contractional forces in the upper plate (Handler et al. 2004).

The Upper Cretaceous section is overlaid, along a parallel unconformity, by coarse-grained continental deposits of the latest Maastrichtian to early Paleocene (Danian) age based on palynological analysis (Zagorchev et al. 2001; Pavlishina 2002; Boyanov et al. 2003). The sediments consist mainly of polymict conglomerates with clasts of Upper Cretaceous volcanic, intrusive and sedimentary rocks, as well as Paleozoic granitoids and high-grade metamorphic rocks (Zagorchev et al. 2001). Sandstones containing abundant coalified plant debris (Pavlishina 2002; Boyanov et al. 2003) and coal-bearing siltstones are also present (Boyanov et al. 2003).

Late Alpine phase

The main Late Alpine compressional event in the Sredna Gora Zone was related to the closure of the intra-arc/back-arc basins at the end of the Maastrichtian and the following until middle Eocene tectonics that led to the formation of mostly NW–SE trending regional fold and fault structures (Bončev 1940; Bergerat et al. 2010; Ivanov 2017). The most prominent Late Alpine faults related to the evolution of the Panagyurishte basin are Panagyurishte, Krasen and Stefanchovo faults (Fig. 2). The last one is interpreted as a south-eastern continuation of the Kamenitsa–Rakovitsa fault zone, situated north-west of the studied region (Gerdjikov et al. 2019, 2020; Kounov & Gerdjikov 2020). These faults were reported as thrusts (Karagjuleva et al. 1974; Gerdjikov et al. 2020; Kounov & Gerdjikov 2020) or dextral oblique reverse structures (Ivanov et al. 2017; Balkanska et al. 2018; Balkanska & Georgiev 2020). Along these structures the crystalline basement, together with its Triassic sedimentary cover, was thrust over different parts of the Upper Cretaceous–Paleocene sediments. Kounov & Gerdjikov (2020) interpreted the Panagyurishte and Krasen faults as extensional structures controlling the Paleocene deposition, which later were inverted during the subsequent compression. The only age constraints of this tectonic event were reported by Handler et al. (2004). Some of their $^{40}Ar/^{39}Ar$ analyses presented low-energy release steps at ca. 40–32 Ma which were interpreted as weak thermal overprint during the Eocene–early Oligocene related to final stages of the crustal shortening in the central parts of the Sredna Gora Zone.

Cenozoic extension

The following Cenozoic evolution of the central parts of the Sredna Gora Zone is still not well constrained. It is related to the opening of the Thrace basin since the Bartonian time and formation of numerous extensional faults bounding several second rank grabens and other structures, filled with Bartonian to Quaternary predominantly terrigenous continental deposits with subordinate marine sediments (Sapoundjieva & Dragomanov 1991; Popov et al. 2015).

Fission-track thermal modelling of samples from the crystalline basement in the northern part of the Sredna Gora Zone at the foot of the Stara Planina Mountains revealed a phase of increased cooling and exhumation between ~44 and 30 Ma, probably related to the syn- to post-orogenic collapse coeval

with the earliest stages of the Cenozoic extension in the region (Kounov et al. 2018).

Low-temperature thermochronological analysis

Sampling strategy

Nine rock samples were collected for $^{40}Ar/^{39}Ar$ and apatite and zircon fission-track dating along two traverses in the central parts of the Sredna Gora Zone. The first traverse transects the crystalline basement outcropping along the slope of the highest parts of the Sredna Gora Mountains between the town of Panagyurishte and Bogdan peak (Koprivshtitsa traverse), whereas the second traverse crosses the Panagyurishte basin (Panagyurishte traverse, Fig. 2, Tables 1, 2 and Supplementary Table S1).

Five granitic samples from the Koprivshtitsa traverse (Fig. 2) were collected at different altitudes (between 565 m and 1604 m), along a tectonically uninterrupted segment, in order to constrain the cooling history of the Variscan basement and estimate its exhumation rate. Sample SG1 (from the Karavelovo pluton) represents biotite granite and was taken from the highest summit of the Sredna Gora Mountains (peak Bogdan, 1604 m). Two-mica granitic samples SG2 and SG3 of the Smilovene pluton were collected from 1327 m and 917 m altitudes, respectively. The lowermost samples (SG4 and SG9) taken at about 500 m altitude, near the border of the Panagyurishte basin, belong to the Streltcha muscovite granitic pluton. One of the samples (SG9) lacks apatites of sufficient quality (which means without fractures and inclusions), hence only zircons were further analysed for fission-track dating.

Four samples were collected across the Panagyurishte traverse in order to constrain the thermal and tectonic evolution of the inverted basin (Fig. 2). Three of them are from the Upper Cretaceous volcanic and subvolcanic rocks, whereas one is from the upper Maastrichtian–Danian conglomerates. The location of the samples is close to two main fault structures in the studied region – Krasen and Stefanchovo faults (Fig. 2). Sample SG5 was taken from the hanging wall, and sample SG6 – from the footwall of the high-angle Krasen thrust, whereas samples SG8 and SG7 were taken from the hanging- and the footwall of the high-angle Stefanchovo thrust, respectively.

Analytical procedures

$^{40}Ar/^{39}Ar$ method

Biotite and muscovite from two samples from the granitic basement (SG1 and SG9) and biotite from one sample from the Upper Cretaceous volcanic rocks (SG7) were separated for $^{40}Ar/^{39}Ar$ multiple single grain fusion dating (Suppl. Table S1). All analytical procedures were performed at the Vrije Universiteit of Amsterdam. The samples were packed in a 9 mm aluminium package and loaded with the in-house Drachenfels sanidine standard in 25 mm aluminium cups. Samples and standards were irradiated for 18 hours in the OSU TRIGA CLICIT position in irradiation batch VU118. After irradiation, samples and standards were unpacked and loaded in a 185 (~3 mm^2) holes of a Cu tray. This tray was prebaked for 24 hours in a vacuum at 250 °C and consecutively placed in the sample chamber connected to a Helix MC mass spectrometer and baked at 120 °C. A 25 W Synrad CO_2 laser was used for fusing the standards and samples in one step. The released gas was purified using the Lauda cooler at 70 °C, a NP10 at 400 °C, ST172 at 400 °C and Ti sponge at 500 °C. The cleaned gas was expanded into a ThermoFisher Helix multi-collector mass spectrometer and ^{40}Ar is measured on the H2-Faraday cup, ^{39}Ar on the H1-Faraday cup, ^{38}Ar on the AX-CDD, ^{37}Ar on the L1-CDD, and ^{36}Ar on the L2-CDD (CDD=compact discrete dynode).

Data reduction was performed off-line using the ArArCalc software (Koppers 2002). Ages were calculated relative to Drachenfels sanidine of 25.522±0.078 Ma based on Wijbrans et al. (1995) and recalibrated relative to Kuiper et al. (2008). Decay constants of Min et al. (2000) were used. The atmospheric $^{40}Ar/^{36}Ar$ ratio of 298.56±0.31 is based on Lee et al. (2006). The correction factors for neutron interference reactions are $(2.64\pm0.02)\times10^{-4}$ for $(^{36}Ar/^{37}Ar)_{Ca}$, $(6.73\pm0.04)\times10^{-4}$ for $(^{39}Ar/^{37}Ar)_{Ca}$, $(1.21\pm0.003)\times10^{-2}$ for $(^{38}Ar/^{39}Ar)_{K}$ and $(8.6\pm0.7)\times10^{-4}$ for $(^{40}Ar/^{39}Ar)_{K}$. Samples were corrected for gain using peak jumping of m/e 44 in dynamic mode on all collectors and gain was calculated relative to AX-CDD. Gain was

Table 1: Zircon fission-track data.

Sample number	Latitude	Longitude	Elevation (m)	Lithology	Stratigraphic/ Absolute age	No. of counted grains	Ns	ps (10^6cm^{-2})	238U (ppm)	P(χ2) %	T pooled ± 1 σ (Ma)	T central ± 1 SE (Ma)
SG 1 (Bogdan)	42.6072	24.4615	1604	Bi granite	Carboniferous	8	413	10.9	245.3	0.05	82.6±5.1	**84.8±5.8**
SG 3 (Ks 17-920)	42.5685	24.3408	917	two-mica granite	Carboniferous	6	300	10.7	227.2	0.02	87.8±6..3	**90.3±7.0**
SG 7 (Stiptsata)	42.4269	24.1944	472	granite porphyry	Upper Cretaceous	5	273	10.1	227.6	2.09	82.8±6.3	**85.1±7.0**
SG 9 (Ks-520)	42.49323	24.28033	521	Mus granite	Permian	9	423	11.1	259.3	0.14	80.0±4.8	**82.2±5.5**
SG 6 (S 17-26)	42.445	24.2758	556	conglomerates	Upper Maastrichtian–Danian	9	373	8.7	125	0	128.9±8.6	**132.9±9.7**

Ns – number of spontaneous tracks counted; ps – spontaneous track density; 238U – pooled mean concentration of Uranium-238, The uncertainty of 238U was estimated at 10 % based on repeated measurements of NIST 610 and NIST 612 standards (Hasebe et al. 2004); P(χ2) – the chi-square probability for pooled age;
T pooled and T central – pooled mean age and central age, respectively

Table 2: Apatite fission-track data.

Sample number	Latitude	Longitude	Elevation (m)	Lithology	Tectonic unit	Stratigraphic/ Absolute age	No. of counted grains	Ns	ps (10^6 cm^{-2})	238 U (ppm)	P(χ2) %	T pooled ± 1 σ (Ma)	T central ± 1 SE (Ma)	No. of lengths measured	MTL (μm)	Std. Dev. (μm)	STERR (μm)	Dpar (μm)
Koprivshtitsa section																		
SG 1 (Bogdan)	42.6072	24.4615	1604	Bi granite	Central Sredna Gora basement	Carboniferous	25	1231	2	91.5	88.96	43.1±1.5	**41.6±2.6**	83	14.04	1.38	0.16	1.32
SG 2 (Barikadi)	42.5717	24.4605	1327	two-mica granite	Central Sredna Gora basement	Carboniferous	24	357	0.7	31.4	60.8	42.6±2.4	**41.2±3.2**	113	13.76	1.54	0.14	1.3
SG 3 (Ks 17-920)	42.5685	24.3408	917	two-mica granite	Central Sredna Gora basement	Carboniferous	20	391	1	44.6	96.33	42.1±2.4	**40.6±3.1**	28	13.11	1.5	0.28	1.28
SG 4 (Pan 650)	42.5248	24.1949	565	Mus granite	Central Sredna Gora basement	Permian	15	367	1.7	82.6	62.38	40.8±2.4	**39.4±3.1**	46	12.82	2.12	0.31	1.46
Panagyurishte section																		
SG 5 (B9)	42.4647	24.2789	650	dacite	Panaguirishte basin	Upper Cretaceous	21	123	0.2	6.4	93.83	72.2±6.7	**70.3±7.5**	38	14.61	1.38	0.22	2.51
SG 6 (S-17-26)	42.445	24.2758	556	conglomerates	Panaguirishte basin	Upper Maastrichtian–Danian	29	1552	1.7	48.5	59.59	69.3±2.2	**67.0±4.1**	49	13.97	1.22	0.17	2.35
SG 7 (Stiptsata)	42.4269	24.1944	472	granite porphyry (Elshitsa pluton)	Panaguirishte basin	Upper Cretaceous	21	287	0.3	7.7	50.07	77.0±4.9	**75.0±6.2**	24	13.74	1.44	0.17	2.69
SG 8 (Tarnichevo)	42.4105	24.2164	706	granite porphyry (Elshitsa pluton)	Panaguirishte basin	Upper Cretaceous	16	84	0.5	10.2	93.52	87.3±9.8	**84.6±10.5**	46	14.65	0.84	0.13	1.88

Ns – number of spontaneous tracks counted; ps – spontaneous track density; 238U – pooled mean concentration of Uranium-238. The uncertainty of 238U was estimated at 10 % based on repeated measurements of NIST 610 and NIST 612 standards (Hasebe et al. 2004); P(χ2) – the chi-square probability for pooled age; T pooled and T central – pooled mean age and central age, respectively; MTL – mean track length; Std. Dev. – standard deviation; STERR – strandard error; Dpar – long axis of track etch pit

measured before and after the tray was measured. Gain correction factors and their standard errors are 0.96664±0.00014 for H2-Far, 0.99550±0.00014 for H1-Far, 1.00570±0.00006 for L1-CDD, and 0.98580±0.00014 for L2-CDD. Errors are quoted at the 2σ level and include all analytical errors. All relevant analytical data for age calculations are given in Suppl. Table S1.

The bulk values of closure temperatures (Tc) of analysed mineral phases, estimated using experimentally derived diffusion parameters, are at ca. 405 °C for muscovite (at 5 kbar, Harrison et al. 2009), and ca. 310 °C for biotite (Harrison et al. 1985) at moderate cooling rates (ca. 10 °CMa^{-1}).

Fission-track method

The samples were processed and analysed in the newly established Low-Temperature Thermochronology Laboratory in Bulgaria, situated in Sofia University and the Geological Institute, Bulgarian Academy of Sciences. At least 100 apatite and zircon grains (where present) were separated by standard mineral separation procedures. The apatite grains were mounted in epoxy resin and the zircons in PFA (tetrafluoroethylene) Teflon sheets. After mounting, the mounts were proceeded to pre-grinding, grinding and polishing. The apatites were etched in 5.5 M HNO_3 for 20 s at temperature of 21 °C. The zircon mounts were etched in an eutectic mixture of KOH:NaOH in Teflon cups in an oven at temperature of 230 °C for 14–24 hours in two or more steps. The counting and measurements of spontaneous tracks was carried out at Sofia University under a Leica DM 2500 POL optical microscope using ×100 dry objective with a total magnification of ×1000. Five measurements of the diameters of etch pits parallel to the crystallographic c-axis (Dpar) were made on each counted or measured grain as a proxy for compositional influence on annealing (e.g. Carlson et al. 1999). For calculation of ^{238}U concentration, LA–ICP–MS technique was used. Fission-track ages and errors were calculated by the equation of Hasebe et al. (2004). Zeta calibration approach (Hasebe et al. 2013) was applied based on Fish Canyon Tuff apatite and zircon standards (Gleadow et al. 2015) and Nisatai Dacite zircon used as a standard by Tagami et al. (1995). The detailed analytical techniques and procedures are described in Balkanska et al. (2021). Summary of apatite and zircon fission-track data for the used age standards obtained by using absolute calibration (Hasebe et al. 2004) is given in the Appendix.

The temperature range within which partial track annealing (i.e. partial resetting) occurs is known as the partial annealing zone (PAZ). The effective closure of the system lies within this PAZ and depends on the overall cooling rate and kinetic properties of the host mineral. The specific PAZ for apatite lies between 60 and 120 °C (Green & Duddy 1989; Corrigan 1993), with a mean effective closure temperature of 110±10 °C (Gleadow & Duddy 1981).

The knowledge of zircon annealing is less advanced and a wide-range of temperature intervals has been published for the partial annealing zone of zircon. Yamada et al. (1995)

suggested temperature limits of ~390–170 °C, whereas Tagami and Dumitru (1996) and Tagami et al. (1998) suggested temperature limits of ~310–230 °C. In his overview on the zircon fission-track method, Tagami (2005) reported temperature ranges for the closure temperature between ~300–200 °C and Yamada et al. (2007) ~350–260 °C respectively. Accordingly, we use a value of ~300 °C for the mean effective closure temperature and 250–350 °C temperature interval for the PAZ.

$^{40}Ar/^{39}Ar$ data

The results from $^{40}Ar/^{39}Ar$ single-grain fusion analyses are presented in Suppl. Table S1 and Fig. 3. For every sample totally 12 mica grains were analysed. In sample SG7 ages range from 93.6 to 87.2 Ma. Most of the grains in this sample have low K/Ca ratios (<1), suggesting very strong alteration of the measured biotite minerals. Two grains have biotite K/Ca ratios of ~9.8 and 6.4 and yield ages at 88.17±0.35 Ma and 88.33±0.18 Ma, respectively. The total fusion experiment of this sample (Fig. 3a) produces a weighted mean age, calculated from the 7 youngest grains, of 88.0±0.30 Ma (MSWD 6.29, inverse isochron age 87.22±1.26) with an initial $^{40}Ar/^{36}Ar$ estimate of 315.38±26.43.

The analysed grains from sample SG1 yield ages between 139.6 and 120.6 Ma (Suppl. Table S1). The total fusion experiment on biotite from this sample (Fig. 3c) produces a weighted mean age of 130.90±3.96 Ma (MSWD 1092.40, inverse isochron age 145.77±10.06) with an initial $^{40}Ar/^{36}Ar$ estimate of 189.28±122.48.

The ages of the muscovite grains in sample SG9 range from 279.6 to 137.6 Ma (Suppl. Table S1). The total fusion experiment of grains from this sample (Fig. 3b) produces a weighted mean age of 225.76±29.69 Ma (MSWD 67578.40, inverse isochron age 54.26±27.68) with an initial $^{40}Ar/^{36}Ar$ estimate of 8268.75±7325.65.

Zircon fission-track data

The results of the zircon fission-track analyses are presented in Table 1. The quality of most of the zircon grains was insufficient for track counting due to zonation of track densities, abundance of inclusions and/or high density of tracks. Consequently, FT zircon ages were obtained for only five samples, using between 5 and 9 grains.

The obtained zircon FT ages of four of the samples range between 90.3±7.0 and 82.2±5.5 Ma (Fig. 2, Table 1). These samples did not pass the Chi-square (χ^2) test and considering the low number of grains, the obtained data are regarded only as an approximation of the true zircon FT ages and therefore will be used further in the discussion with caution.

The sample from the upper Maastrichtian–Danian conglomerates (SG6) also did not pass the Chi-square (χ^2) test, probably due to multiple detrital grain populations. Three groups of single grain ages were distinguished in the population of nine analysed grains from this sample (Fig. 4). One grain yields FT age of 342±58.1 Ma (Fig. 4), four yield ages between 148.3±24.7 Ma and 129.4±23.1 Ma and the youngest four grains yield ages between 91.9±25.4 Ma and 80.2±12.3 Ma.

Apatite fission-track data

The results of the apatite fission-track analysis are presented in Table 2. For each sample between 15 and 29 single apatite grains were used for the age calculation. The reported confined mean track lengths represent un-projected onto c-axis values. The samples from the Koprivshtitsa traverse yield apatite FT ages between 41.6±2.6 Ma (SG1, the topographically highest sample) and 39.4±3.1 Ma (SG4, the topographically lowest sample). In all four apatite samples horizontal confined tracks and corresponding C-axis angles were measured. For each sample between 28 and 113 track lengths were measured (Table 2). The confined mean track lengths are between 12.82 and 14.04 μm with standard deviation between 1.38 and 2.12 μm. The Dpar values vary from 1.28 μm to 1.46 μm (with standard deviation of approx. 0.50 μm). The single grain age distributions are shown on Fig. 5. All four samples pass the Chi-square (χ^2) test (Table 2). The age-altitude diagram of the samples from the Koprivshtitsa traverse based on the obtained results is given on Fig. 6.

The Upper Cretaceous volcanic and plutonic rocks from the Panagyurishte traverse yield apatite FT ages between 84.6±10.5 Ma and 70.3±7.5 Ma. The upper Maastrichtian–Danian sediments from the Panagyurishte basin yield apatite FT age of 67.0±4.1 Ma. All four samples pass the Chi-square (χ^2) test (Table 2). The confined mean track lengths of the samples from Panagyurishte traverse are between 13.74 μm and 14.65 μm with standard deviation between 0.84 and 1.44 μm. The Dpar values vary from 1.88 μm to 2.69 μm (with standard deviation of approx. 0.70 μm). The single grain age distributions of the samples from this traverse are shown on Fig. 5.

Fission-track thermal history modelling

Our first intention was to use one single modelling software for all analysed samples in order to avoid any possible doubts for potential bias of the results due to the differences in the inverse modelling algorithms (HeFTy and QTQt, see the discussion in Vermeesch & Tian 2014). However, the modelling of the samples with both HeFTy (Ketcham 2005) and QTQt (Gallagher 2012) softwares gave several differences in their statistical probability and geological credibility results. It is important to remember here that the best thermal history obtained during the modelling process is not necessarily the only possible. Other thermal histories may match the observed data and it is therefore imperative to consider as many geological constraints as possible to determine the most likely path. Therefore, we finally chose the thermal models that match better the observed data and correspond to a greater extent to the already known constraints in the geological evolution of the studied area.

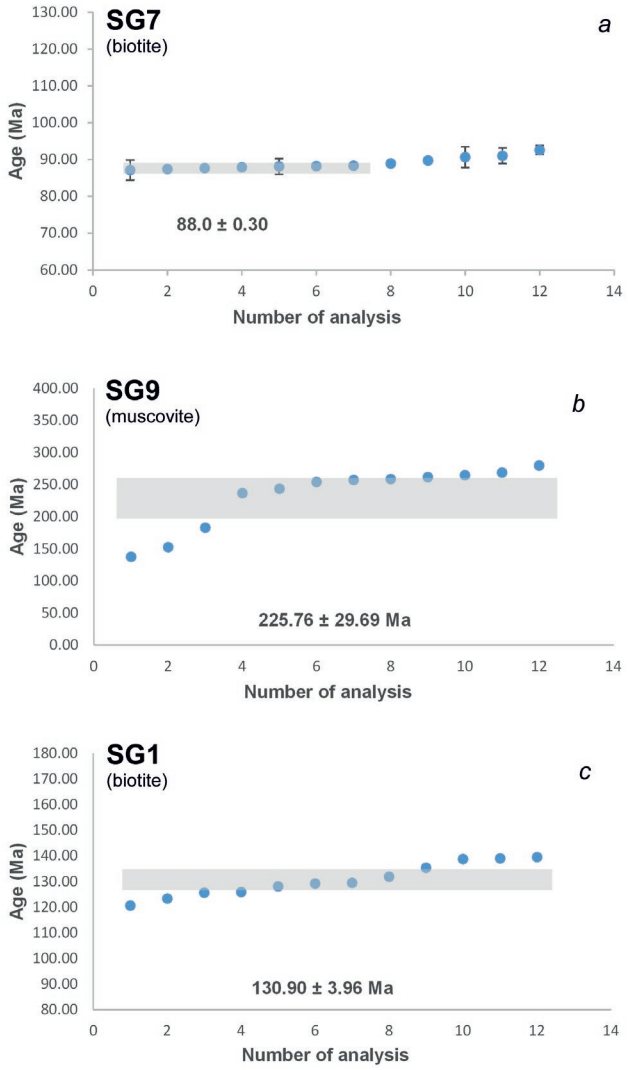

Fig. 3. $^{40}Ar/^{39}Ar$ total fusion ages for samples SG7 (**a**), SG9 (**b**) and SG1 (**c**). Weighted mean ages are reported with 2 σ errors. Data outside the enclosed area in (a) are not included in the weighted mean age.

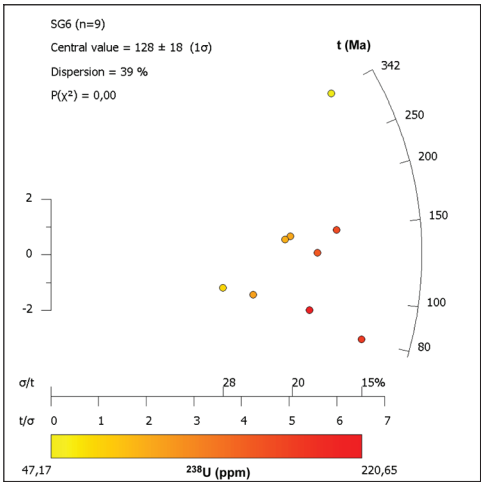

Fig. 4. Distribution of the zircon fission track single grain ages of sample SG6.

Koprivshtitsa traverse

Thermal history modelling for the Koprivshtitsa traverse was performed using a Bayesian multi-sample vertical profile inversion approach of the QTQt software (Gallagher 2012). This method allowed us to analyse the four Carboniferous granitic samples simultaneously and produce a time-temperature model of the whole traverse. We adopted the multi-compositional fission-track annealing model of Ketcham et al. (2007) and used the Dpar kinetic parameter as a proxy for the chemical composition of the apatites (Carlson et al. 1999). Input parameters also included apatite fission-track single grain ages and measured individual C-axis projected track lengths. Time-temperature constraint boxes for two time intervals were assigned in the model. The first one between 100 and 90 Ma at 220±80 °C corresponds to the period of Late Cretaceous magmatism in the area, while the other one between 60 and 20 Ma at 100±60 °C reflects the expected period of post orogenic exhumation related to regional extension. The expected thermal history model (weighted mean model) shows a period of relatively fast cooling between 45 and 39 Ma (Fig. 7a), whereas the maximum likelihood thermal history model (best fitting model) predicts a rapid cooling episode at 44.5–42.2 Ma followed by moderate cooling between 33.5 and 27.5 Ma (Fig. 7c). These two cooling events are separated by a period of relative quiescence during which the samples remain at temperatures between 60 and 50 °C. Summaries of the observed and predicted values of apatite fission-track parameters of the single samples for the two models are given on Fig. 7b and 7d.

Panagyurishte traverse

For modelling of the samples from the Panagyurishte traverse we used HeFTy software (Ketcham 2005), which was more effective in assessing the thermal history of the single samples. Input parameters include apatite FT ages, track-length distributions and Dpar values. To define the Cenozoic thermal history of each sample, we used the "best-fit path" (black lines on Fig. 8), which corresponds to the statistically best fit between measured and modelled data. As time–temperature constraints (t–T) for samples SG5, SG7 and SG8 (the volcanic and subvolcanic rocks in the Panagyurishte basin) we chose three boxes (Fig. 8). The two smaller boxes correspond to the emplacement age of these igneous rocks (in the interval 90–80 Ma) and the expected time at which they were exposed on the surface (90–65 Ma). The third large t–T box was chosen in order to give the model more freedom to search for possible solutions from the end of the Cretaceous to recent times.

Although we have obtained a relatively small number of confined horizontal track lengths from the volcanic and

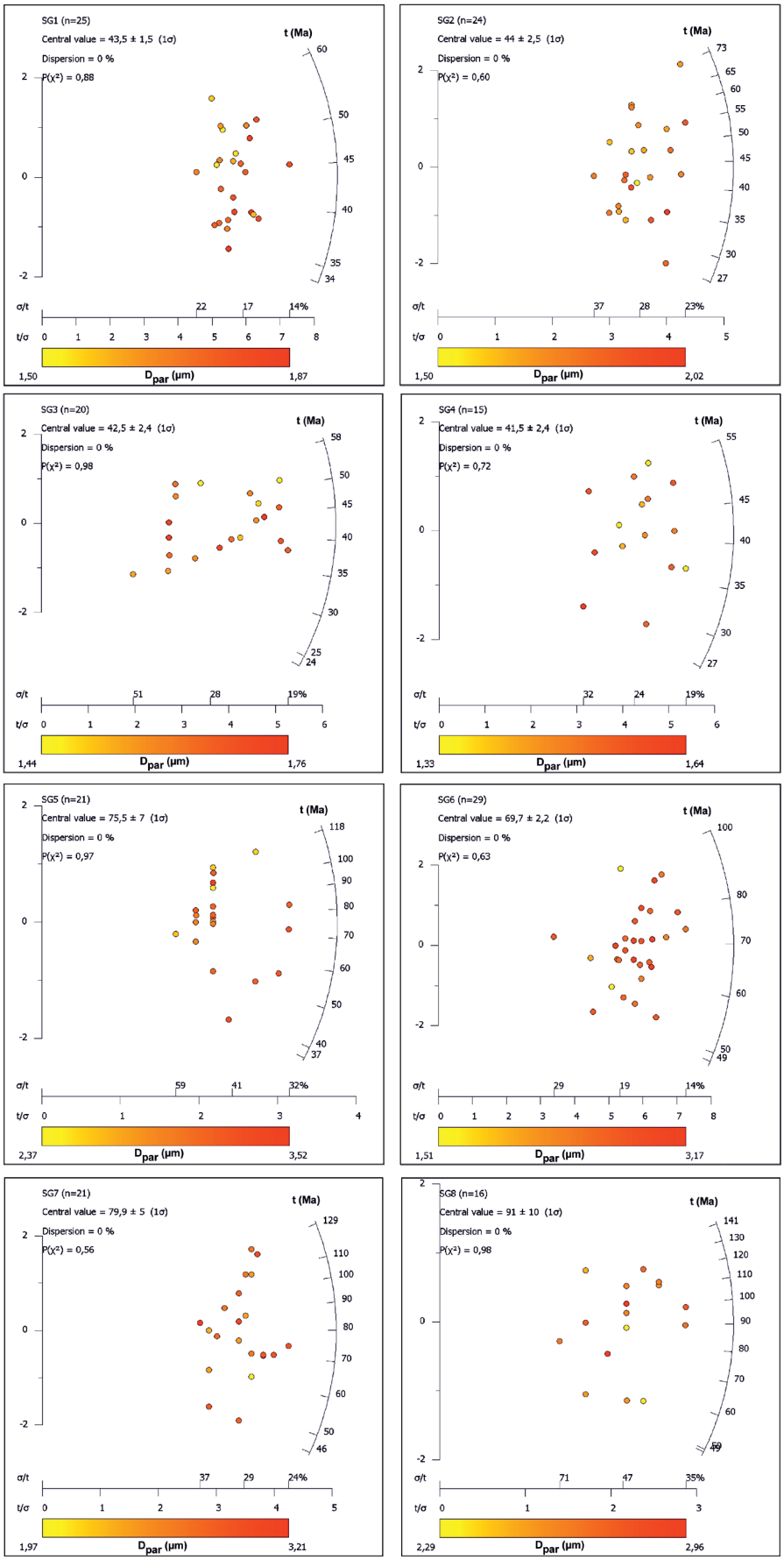

Fig. 5. Radial plots presenting the distribution of the apatite fission track single grain ages for all samples using RadialPlotter (Vermeesch 2018).

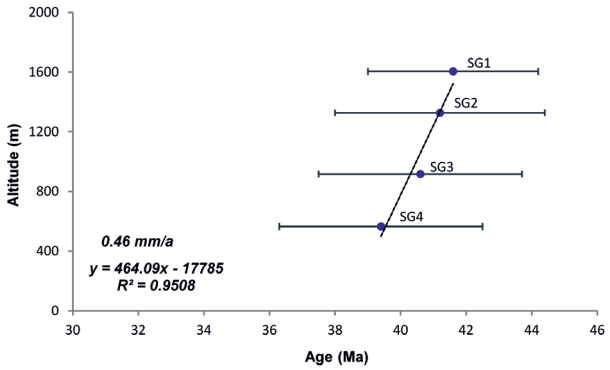

Fig. 6. Age-altitude diagram of the apatite FT ages (with 1σ errors) of the samples from the Koprivshtitsa traverse.

subvolcanic rocks, the thermal modelling of these samples revealed a thermal evolution that is supported by the other thermochronological data and the geological evidence discussed in the next section. They are also similar to the results of the sedimentary sample (SG6) from which the maximum number of track lengths were obtained on this traverse (N=49, Fig. 8). Although there is no general agreement on the minimum number of confined horizontal track lengths necessary to obtain geologically meaningful and statistically robust modelling, some previous studies show that even 40 track lengths can be considered sufficient for reconstruction of the thermal evolution of a sample with relatively complex thermal history (e.g. Rahn & Seward 2000).

The thermal models of the volcanic and subvolcanic samples SG5 and SG7 are similar (Fig. 8). They reveal very rapid

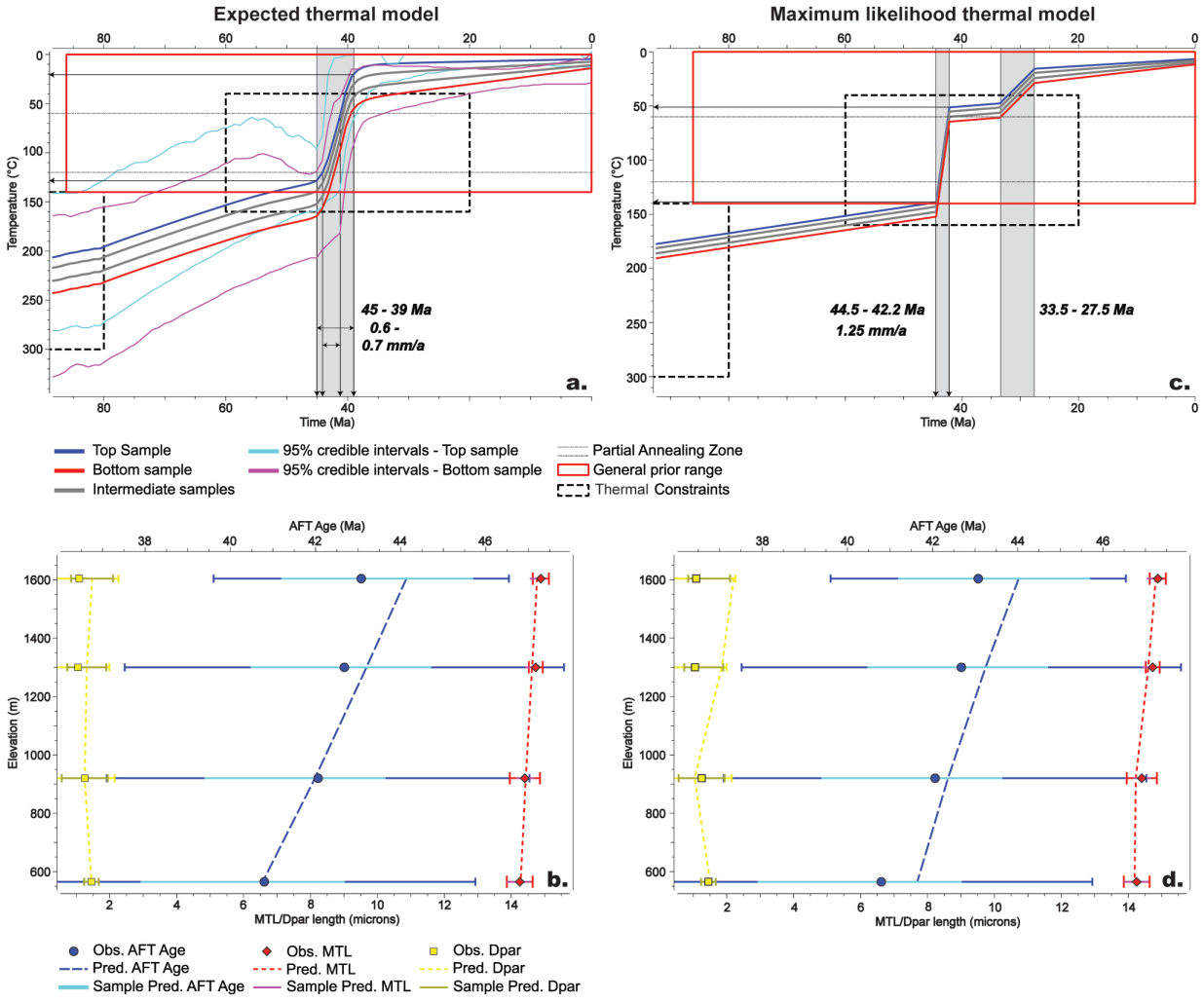

Fig. 7. Thermal history models of the samples from the Koprivshtitsa traverse using QTQt software (Gallagher 2012): **a** — expected thermal model; **b** — summary of observed and predicted values of AFT parameters of the single samples in the expected thermal model; **c** — maximum likelihood thermal model; **d** — summary of observed and predicted values of AFT parameters of the single samples in the maximum likelihood model. The given constraints in the thermal models are drawn as black dotted line boxes. Obs. AFT Age=observed apatite fission-track age; Pred. AFT Age=predicted apatite fission-track age; Sample Pred. AFT Age=95 % credible range of predictions of AFT ages; Obs. MTL=observed mean track lengths; Pred. MTL=predicted mean track lengths; Sample Pred. MTL=95 % credible range of predictions of mean track lengths; Obs. Dpar=observed values of Dpar; Pred. Dpar=predicted values of Dpar; Sample Pred. Dpar=95 % credible range of predictions of Dpar.

cooling to surface temperatures at ~80 Ma after their formation and a subsequent period of burial and reheating between 65 and 55 Ma, followed by moderate to rapid cooling prior to 50 Ma. The model of sample SG5 suggests heating to higher temperatures (~100–120 °C) than the one of sample SG7 (~60 °C). The model of sample SG8 reveals very rapid cooling to surface temperatures soon after its emplacement. No subsequent heating events were suggested by the model.

Three time-temperature constraint boxes were assigned during the modelling of sample SG6 (upper Maastrichtian–Danian conglomerates, Fig. 8). The first small box was set in the interval 90–80 Ma, which corresponds to the emplacement age of the magmatic and volcanic rocks as well as the zircon FT ages obtained from the crystalline basement rocks in the area that all served as a source for these deposits. The second box was set to surface temperatures (between 0 °C and 30 °C) at ~70 to 60 Ma which corresponds to the deposition age of the sediments. The third large box is the same as the one for the other three samples on this traverse. The thermal model of this sample reveals heating to ~70 °C between 65 and 55 Ma followed by moderate cooling to surface temperatures between 55 and 50 Ma.

Interpretation and discussion

Early Alpine thermal evolution

The $^{40}Ar/^{39}Ar$ analysis of the two samples from the granitic basement of the central parts of the Sredna Gora Zone show large single grain age distribution (Figs. 3 and 9) which makes their weighted mean ages highly unreliable.

The muscovite sample SG9 yielded single grain ages between 279.64 and 137.63 Ma (Suppl. Table S1, Fig. 3). The weighted mean age of the sample 225.76±29.69 Ma could not be related to a certain thermal event in the study area and the MSWD value (67578) exceeds the acceptable goodness-of-fit criteria. Neither the Strelcha pluton in general nor the analysed sample show any evidence for ductile deformation or recrystallization (Dabovski et al. 1966; Katskov & Iliev 1993) and thus, the dated muscovite minerals are considered as magmatic. The emplacement age of the Strelcha pluton at 289.5±7.8 Ma (HR–SIMS U–Th–Pb zircon dating, Carrigan et al. 2005) is very close to our maximum age of sample SG9 (older single grain age of 279.64±0.36 Ma, Suppl. Table S1). Therefore, we infer that all grains that yield younger ages than the emplacement age of the granite, underwent differing amounts of partial argon loss. Since the minimum age is 137.63±0.38 Ma (Suppl. Table S1), we could suggest that the radiogenic argon loss was caused by a thermal event at or younger than 137 Ma (Fig. 9).

The other granitic sample (SG1) yield single grain ages between 139.57 and 120.64 Ma. The analysed biotite from the Carboniferous Karavelovo granite is also defined as magmatic since no evidence of metamorphism and deformation could be observed in either the granite or the sample. Therefore, we consider all the dated biotite grains from this sample as fully reset during the thermal event at or before 139.57±0.29 Ma (maximum age, Suppl. Table S1), which partially reset the muscovite from sample SG9. On the other hand, the relatively large age span of the single-grain ages is interpreted as related to another thermal event which led to some partial argon loss probably at or after 120.64±0.35 Ma (minimum age, Suppl. Table S1).

We constrain the peak temperature attained during first thermal event at about 140–138 Ma (Fig. 9) and at temperatures between ~300 and ~400 °C because it obviously fully reset the biotite (closure temperature of 310 °C, Harrison et al. 1985) and partially the muscovite (closure temperature of 405 °C at 5 kbar, Harrison et al. 2009). It must be noticed that the suggested values for closure temperature of these minerals correspond to a moderate cooling rate of ca. 10 °CMa^{-1}. In our particular case, as we are dealing most probably with long lasting thermal events related to relatively lower cooling rates, lower closure temperature ranges could be also expected. Wide ranges of closure temperature values corresponding to different cooling rates were reported for the biotite (~200–350 °C) and the muscovite (~220–400 °C) minerals (e.g. Ehlers et al. 2005). The fact that their partial retention zones overlap, suggests that it is theoretically possible, at certain temperatures, both mineral phases to be partially reset by a thermal event younger than 120 Ma (the biotite minimum age of sample SG1). However, the overlapping range corresponds mostly to closure temperatures of the biotite related to rapid cooling and of muscovite to slow cooling processes which makes their partial resetting during a single thermal event rather unlikely. We have also strong geological evidence for a tectonic and thermal event taking place in the study area at the end of the Jurassic and the beginning of the Cretaceous (Fig. 10A).

Such a thermal event was most probably related to the Early Alpine thrusting in the area (Vangelov et al. 2013; Burchfiel & Nakov 2015; Ivanov 2017), during which the basement rocks of the studied area were tectonically buried below the thrust at the estimated temperatures (Fig. 10A). The hanging wall of the thrust was not preserved, being most probably eroded since that time. It must be noted that the Early Cretaceous compressional tectonic event was not related to a regional metamorphism, but rather to a very low- to low-grade metamorphic overprint in the basement localized to low-grade shear zones (Gerdjikov et al. 2007; Lazarova & Gerdjikov 2008). Our new combined muscovite and biotite $^{40}Ar/^{39}Ar$ single-grain fusion analyses allowed determination of the age at which the rocks of the study area reached peak temperature (Fig. 9). The previously reported step-heating muscovite and biotite $^{40}Ar/^{39}Ar$ plateau ages from the Central Sredna Gora metamorphic basement, taken only 20 km west from the study area, are scattering between 317 and 99 Ma (Velichkova et al. 2004). We now consider most of them to be mixed ages as they do not correspond to any known thermal events in the area or in the neighbouring units.

Further evidence of the Early Alpine Late Jurassic–Early Cretaceous tectonic event in the study area is related to the

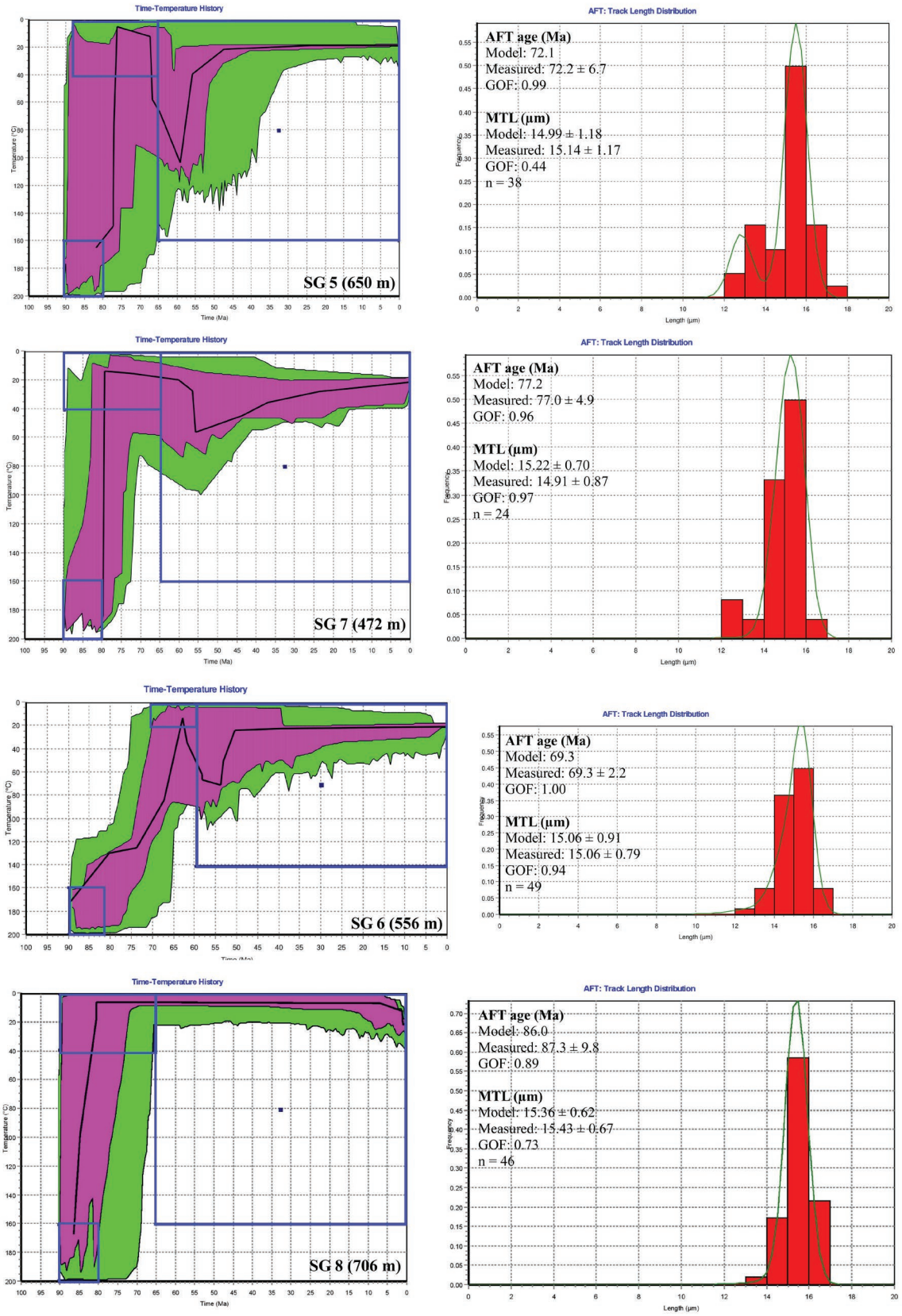

Fig. 8. Thermal modelling results for the samples from the Panagyurishte basin using HeFTy software (Ketcham 2005) with acceptable (green) and good (purple) time–temperature pathway envelopes. The black lines represent the best-fit paths. Time–temperature constraints are given with blue boxes. MTL=mean track length; GOF=goodness of fit value.

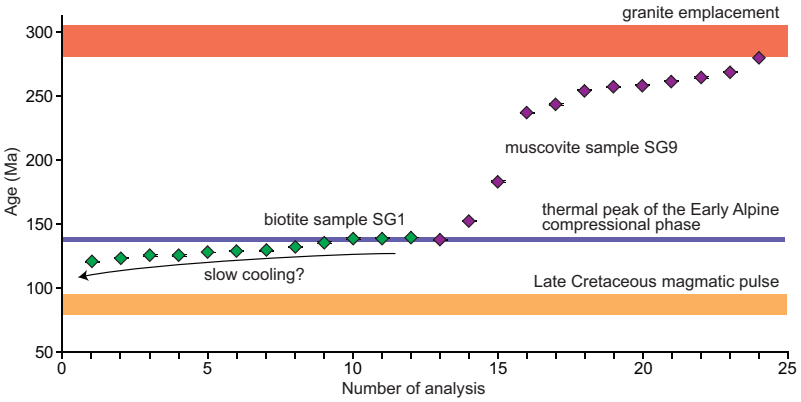

Fig. 9. Interpretation diagram for the thermal evolution of the Sredna Gora Zone granitic basement with presented $^{40}Ar/^{39}Ar$ total fusion single ages of the samples SG1 and SG9.

four detrital grains with ages between 148.3±24.7 Ma and 129.4±23.1 Ma obtained from the upper Maastrichtian–Danian sediments from the Panagyurishte basin (SG6, Fig. 4). These ages suggest that the sediments were sourced by basement rocks that had experienced this Early Alpine event and whose ages reflect cooling related most probably to syn-thrusting erosion or eventually post-thrusting tectonic or erosional processes. Similar Late Jurassic–Early Cretaceous ages have been reported for the syn-metamorphic thrusting in the neighbouring Rhodope and Sakar–Strandja zones (Fig. 1, Kirchenbaur et al. 2012; Bonev et al. 2020; Szopa et al. 2020).

The second thermal event, younger than 120 Ma (Fig. 9) that led to the partial argon loss in the biotite sample SG1, could be related to the Late Cretaceous (between 90 and 86 Ma) magmatic activity in the Sredna Gora Zone (Fig. 1). The zircon FT age of 84.8±5.8 Ma from this sample (Fig. 2, Table 2, SG 1) suggests that the temperature exceeded 300 °C during this thermal event. Another possible interpretation of the results from sample SG1 is a very slow cooling between 139 to 120 Ma (Fig. 9) which would keep the system open for the partial argon loss for a relatively protracted period. Such slow cooling could be related to the erosion of the thrust sheets during the ongoing compression which probably continued until the Aptian (Ivanov 2017).

Thermal evolution of the Panagyurishte basin and its basement

Late Cretaceous

The Late Cretaceous in the studied area was a time for formation of the intra-arc/back-arc Panagyurishte basin accompanied by volcanic activity (Fig. 10B, Aiello et al. 1977; von Quadt et al. 2005). Our combined zircon and apatite FT analyses together with the $^{40}Ar/^{39}Ar$ dating are in agreement with the previous geochronological data on this magmatic and volcanic event in the central parts of the Sredna Gora Zone (Handler et al. 2004; Rieser et al. 2008).

The thermal models of the volcanic and subvolcanic rocks from the Panagyurishte basin (SG5, SG7 and SG8) suggest very rapid cooling to surface temperatures between ~87 and 78 Ma that is in concordance with their supposed Late Cretaceous formation ages (Dimitrova et al. 1984; Popov et al. 2002a; von Quadt et al. 2005; Peytcheva et al. 2009). Although it must be noticed that this cooling is not constrained with the necessary high probability by the modelling programme due to the posterior reheating and partial resetting of the FT data of these samples (see the next section), we consider the event well constrained by the geological evidence. These samples represent volcanic rocks for which fast cooling after their emplacement or eruption must be expected (Fig. 10B).

The obtained $^{40}Ar/^{39}Ar$ weighted mean age of 88.0±0.30 Ma from the granite porphyry (sample SG7) is generally in line with that reported for the Upper Cretaceous magmatic rocks in the study area U–Pb ages between 90 and 86 Ma (Peytcheva et al. 2003, 2008; von Quadt et al. 2005), Re/Os ages between 87.7±0.50 Ma and 86.8±0.50 Ma of hydrothermal molybdenite from quartz veins in the Elshitsa shallow intrusive porphyritic rocks (Vlaykov Vrah, Zimmerman et al. 2008), as well as with other $^{40}Ar/^{39}Ar$ post-magmatic cooling ages from volcanic and plutonic rocks from the Panagyurishte basin (between 91 and 84 Ma, Handler et al. 2004; Rieser et al. 2008).

However, the $^{40}Ar/^{39}Ar$ age of 88.0±0.30 Ma is slightly older than the U–Pb zircon age of 86.61±0.31 Ma reported for the Elshitsa pluton (Peytcheva et al. 2008). The sampled small subvolcanic body is spatially and genetically related to this pluton and therefore considered as part of its hypabyssal facies. One possible reason for this increasing of the $^{40}Ar/^{39}Ar$ age could be the apparent strong replacement of the biotite by chlorite, as suggested by the low K/Ca ratios (<1, Suppl. Table S1) for most of the analysed grains. The $^{39}Ar_K$ recoil from the biotite layers, alternating with the chlorite ones in the altered mineral, during neutron irradiation could lead to producing an older age than the true formation age of the analysed sample (Lo et al. 2000). Even if the $^{39}Ar_K$ had recoiled from layers of K-rich biotite into layers of K-poor chlorite, argon will be less well-retained by chlorite layers and thus the $^{39}Ar_K$ will be released more quickly than $^{40}Ar^*$, which is located mostly within biotite layers (Shi et al. 2020). Finally, this process will produce low $^{40}Ar^*/^{39}Ar_K$ ratios and therefore older ages.

The obtained zircon FT age of the sample is 85.1±7.0 Ma. Despite the low-number of analysed grains (only 5), this age could be tentatively interpreted as related to the cooling of the rock after its emplacement.

The zircon fission-track ages between 90.3±7.0 and 82.2±5.5 Ma of the samples from the Sredna Gora granitic basement (SG1, SG3, SG9, Fig. 2, Table 2) indicate that

the Paleozoic granites were thermally affected by the Late Cretaceous magmatic event at temperatures higher than 300 °C (Fig. 10B). Hence, these zircon FT results represent the cooling ages of the granitic basement after this thermal event. This cooling could be a direct consequence of a post-magmatic relaxation or exhumation along the northern margin of the Late Cretaceous Panagyurishte basin during its early rifting stage (Fig. 2).

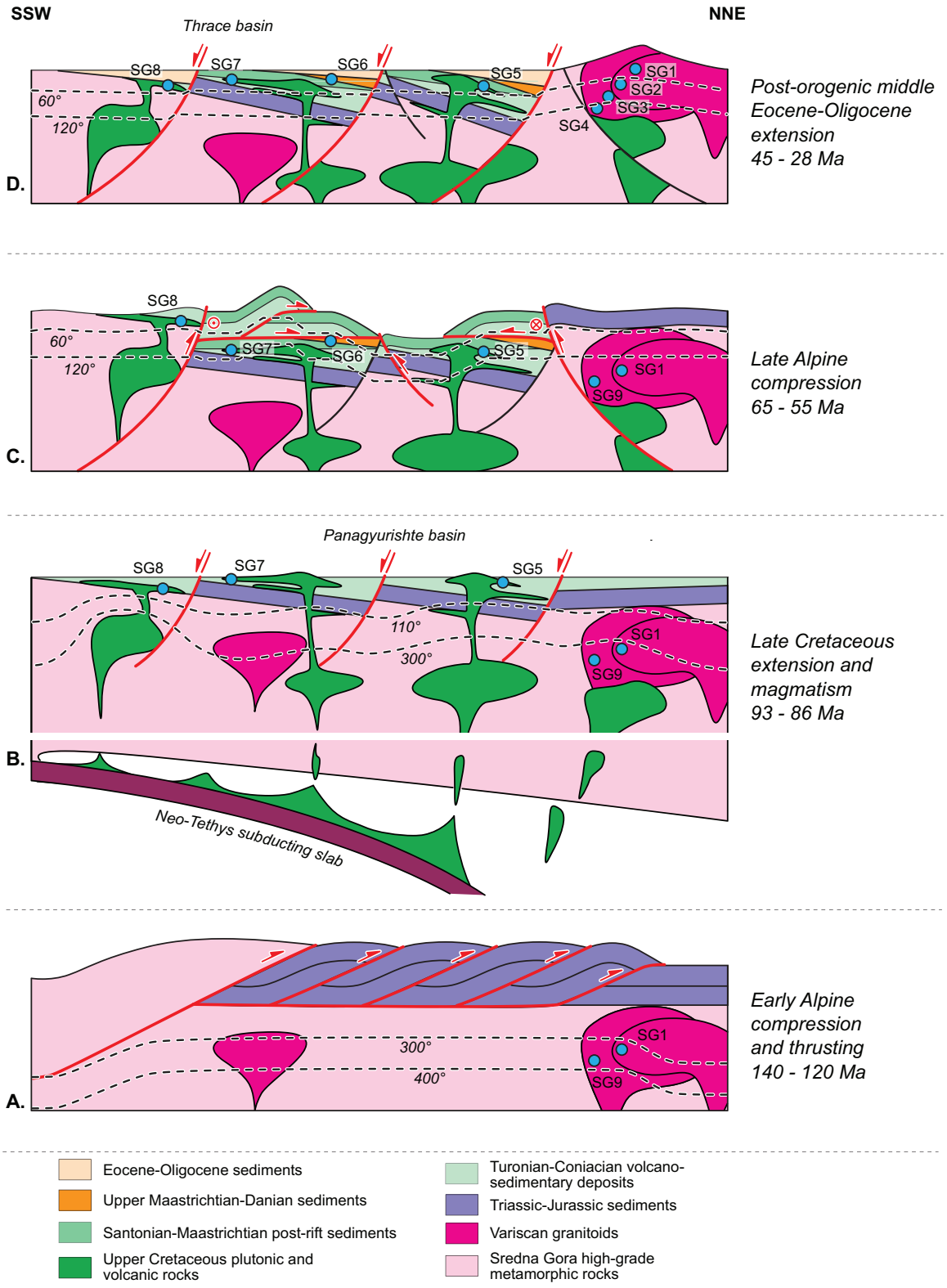

Fig. 10. Schematic evolutionary model of the central parts of the Sredna Gora Zone during Alpine time.

Paleocene

The thermal models of the Upper Cretaceous volcanic and subvolcanic rocks (SG5 and SG7) and upper Maastrichtian–Danian sediments from the Panagyurishte basin (SG6) reveal heating to temperatures within the apatite PAZ (60–120 °C) between 65 and 55 Ma. This thermal event is interpreted as a direct consequence of tectonic burial, probably related to the Late Alpine (post-Danian) compression, which led to the closure of the Panagyurishte basin and formation of the regional fault structures along which the Paleozoic basement and its Mesozoic cover were thrust over the volcano-sedimentary sequences (Karagjuleva et al. 1974; Katskov & Iliev 1993, Fig. 10C). Not all good paths outlining the purple envelope follow the curve of the "best-fit path" (the black line) and some of their trajectories are quite different (Fig. 8). This fact shows that most probably this is not the only possible/acceptable solution for the thermal history of the analysed rocks from the Panagyurishte basin. However, we consider that the obtained "best-fit paths" are the most probable ones not only from statistical point of view but also because they are supported by the geological evidence for the study area and the other thermochronology results. The burial of the upper Maastrichtian–Danian conglomerates is also supported by the fact that the sediments contain abundant coalified plant debris (Pavlishina 2002; Boyanov et al. 2003) and coal-bearing siltstones (Boyanov et al. 2003), which indicate that they have been heated after their deposition. The initiation of the Botev Vrah thrust in the Balkan fold-thrust belt also occurred during the late Paleocene (Balkanska et al. 2012).

Our results exclude the possibility that the thermal event that affected the Upper Cretaceous–lower Paleocene deposits could be related to sedimentary burial. The estimated thickness of the continental upper Maastrichtian–Danian sediments ranges from more than 200 m (Katskov & Iliev 1993) to up to 800 m (Zagorchev et al. 2001; Boyanov et al. 2003) which is insufficient for considerable burial to temperatures allowing for partial resetting of the apatite ages. Although the volume of eroded Paleocene cover could not be estimated, it was previously well established that significant amount of Paleocene sediments in Bulgaria have been deposited only further to the north-east in the foreland basin of the East Balkan zone (Fig. 1, up to 1670 m, Sinnyovski 2004).

The sample SG8 from a small subvolcanic body related to the Elshitsa pluton situated in the hanging-wall of the Stefanchovo thrust fault yielded an apatite FT age of 84.6±10.5 Ma that is quite similar to its supposed emplacement age (U–Pb zircon 86.61±0.31 Ma from the granites of the Elshitsa pluton, Peytcheva et al. 2008). This age clearly represents post-emplacement cooling to temperatures below 60 °C. The thermal model excludes subsequent reheating, unlike the other samples from the Panagyurishte basin (Fig. 8). This could be explained by the fact that being part of the hanging wall of the Stefanchovo thrust this sample was not buried during the compressional event like the sample SG7 taken from the footwall (Fig. 10C). Therefore, the Stefanchovo fault, bordering the Panagyurishte basin to the south-west, could be considered as one of the main structures controlling the closure and the tectonic burial of the basin infill during the Late Alpine event. The tectonic burial below the thrust sheet probably did not last long and its hanging wall was obviously subjected to erosion soon after its emplacement as suggested by the thermal models of the rocks from the Panagyurishte basin, which have predicted relatively fast cooling between 55 and 50 Ma (Fig. 8). Kounov et al. (2018) reported a period of accelerated cooling, between ~58 and ~48 Ma (late Paleocene–early Eocene) in the Balkan fold-thrust belt, related to rapid denudation of the basement rocks thrust sheets during the compressional tectonics.

Cenozoic evolution of the Sredna Gora Zone basement

In order to constrain the distinct cooling episodes in the central parts of the Sredna Gora Zone crystalline basement and estimate their exhumation rate we have used three different approaches (apatite FT age-altitude plot, QTQt expected thermal history model and QTQt maximum likelihood thermal history model) and the results are presented below.

The first one is based on the age-altitude plot of the calculated apatite FT ages (Fig. 6), which have a slope indicating a moderate exhumation rate of 0.46 mm/year between 42 and 39 Ma. The relationship between fission-track ages and the altitude of samples from an elevation profile are commonly used to determine the exhumation rate (Fig. 10D, Fitzgerald & Malusà 2019 and references therein). The advantage of this approach is that it does not require the geothermal gradient to be known. However, several assumptions need to be made to ensure that the slope represents the realistic exhumation rate. It must be assumed that all the samples had the same closure temperature and isotherms were horizontal during the exhumation. Additionally, in the case of rapid exhumation which leads to high thermal gradient due to the advection of the isotherms, the slope of the age-elevation profile will overestimate the true exhumation rate (e.g. Fitzgerald & Malusà 2019). Taking in account these issues and consequent uncertainties, the estimated exhumation rate must be considered only as an apparent rate.

In order to determine better the time and amount of the exhumation of the crystalline basement and avoid some of the problems listed above, we have applied FT thermal modelling using the QTQt software (Gallagher 2012, Fig. 7) to the samples from the Koprivshtitsa traverse.

The expected thermal history model, which represents weighted models where the weighting is provided by the posterior probability for each model (Gallagher 2012), predicts a period of relatively fast cooling between 45 and 39 Ma (Fig. 7a). Assuming an average geothermal gradient in orogenic belts of 30 °C/km used as input in the modelling, an exhumation rate of 0.6–0.7 mm/year was obtained for this time period.

On the other hand, the maximum likelihood thermal history model, which represents the best data fitting models of all samples from the profile, shows a rapid cooling episode at

44.5–42.2 Ma and a subsequent moderate cooling between 33.5 and 27.5 Ma (Fig. 7c). However, the rapid exhumation predicted for the first event would induce advection of the isotherms leading to an increased geothermal gradient. Therefore, the estimated exhumation rates of 1.25 mm/year for a geothermal gradient of 30 °C/km (Fig. 7c) could be considered overestimated. The second cooling event at temperatures below 60 °C (i.e. above the PAZ of the apatite) is outside the applicability temperature limit of this method, and is thus considered poorly constrained.

The Bayesian approach, adopted by the QTQt software, favours the simpler models such as the expected model compared to the maximum likelihood model, which is likely to be too complex, resulting in more time-temperature points (Gallagher 2012). However, the best way to judge which model is better representative of the true thermal evolution is to confront their results with the geological evidence of the study area. As we have noticed before there is practically no information for the evolution of the central parts of the Sredna Gora crystalline basement during the Cenozoic. Therefore, we have to compare our results to the tectonic episodes reported in the neighbouring areas.

An Eocene extensional event, that affected the entire Balkan Peninsula (e.g. Burchfiel et al. 2008), was also reported in the neighbouring Balkan fold-thrust belt where it started in the middle Eocene (~44 Ma, Kounov et al. 2018). Early Eocene extension is reported as an early stage of the Aegean extension in the Kraishte Zone and the Rhodope metamorphic complex south of the Sredna Gora Zone (Fig. 1, e.g. Kounov et al. 2004; Antić et al. 2016; Kounov et al. 2020). We also could not exclude the existence of a second exhumation stage during the Oligocene in the studied area as suggested by the maximum likelihood thermal history model (Fig. 7c). This event could be correlated with the extension in the Rhodopes between ~37 and ~33 Ma, resulting in much faster exhumation rates and formation of metamorphic core complexes (Kounov et al. 2015, 2020).

The cooling and exhumation of the Sredna Gora Zone basement could be related to the period of post-orogenic denudation and extension, associated with the formation of the Thrace basin to the south-south-east of the study area (Figs. 1, 2 and 10D). The oldest sediments in the basin are Bartonian (Sapoundjieva & Dragomanov 1991) which suggests that the regional extension and opening of the basin began at ~40 Ma.

Conclusions

The new apatite and zircon fission track dating combined with $^{40}Ar/^{39}Ar$ analysis revealed the following Alpine (post-Triassic) thermal and cooling events related to tectonic processes in the central parts of the Sredna Gora Zone in Bulgaria:

- The thermal peak of the Early Alpine event was constrained at about 140–138 Ma at temperatures between ~300 and 400 °C attained probably during active thrusting.
- The Late Cretaceous arc-related magmatic and volcanic activities in the central parts of the Sredna Gora Zone between 90 and 86 Ma induced an elevated thermal gradient and reheating at temperatures above 300 °C not only in the Panagyurishte basin but also in its neighbouring basement rocks.
- A middle to late Paleocene thermal event between 65 and 55 Ma was related to the Late Alpine thrusting and closure of the Panagyurishte back-/intra arc basin during which the tectonically buried sediments attained temperatures of <120 °C. This was followed by rapid to moderate cooling of the sedimentary and volcanic successions at 55–50 Ma probably during syn-tectonic erosion and denudation of the thrust sheets.
- The exhumation of the central parts of the Sredna Gora Zone crystalline basement took place during one or two stages of post-orogenic middle Eocene to Oligocene extension most probably related to the opening of the Thrace basin.

Acknowledgements: The study is supported by the grant DN 04/9 funded by the National Science Fund, Ministry of Education and Science, Bulgaria.

References

Aiello E., Bartolini C., Boccaletti M., Gocev P., Karagjuleva J., Kostadinov V. & Manetti P. 1977: Sedimentary features of the Srednogorie zone (Bulgaria): an Upper Cretaceous intra-arc basin. *Sedimentary Geology* 19, 39–68. https://doi.org/10.1016/0037-0738(77)90020-3

Antić M.D., Kounov A., Trivić B. et al. 2016: Alpine thermal events in the central Serbo-Macedonian Massif (south-eastern Serbia). *International Journal of Earth Sciences* 105, 1485–1505. https://doi.org/10.1007/s00531-015-1266-z

Antonov M., Gerdjikov S., Metodiev L., Kiselinov Ch., Sirakov V. & Valev V. 2010: Explanatory note to the geological map of the Republic of Bulgaria, scale 1:50 000. Map sheet K-35-37-B Pirdop. *Geocomplex*, Sofia, 1–99.

Balkanska E. & Georgiev S. 2020: Structural analysis of faults related to the Late Cretaceous and Paleocene evolution of the Central Srednogorie zone, Bulgaria. *EGU General Assembly 2020, Abstracts*. https://doi.org/10.5194/egusphere-egu2020-7790

Balkanska E., Gerdjikov I., Vangelov D. & Kounov A. 2012: Thick-skinned compression in Central Balkanides coeval with extension in the uppermost part of the orogen core. In: *Proceedings of International conference "Geological schools of Bulgaria. The school of Prof. Zhivko Ivanov"*, 13–16.

Balkanska E., Vangelov D. & Georgiev S. 2018: Post-magmatic (ore) transpressive deformation controlling the closure of the Late Cretaceous basin – a case study from the Panagyurishte strip, Central Srednogorie Zone, Bulgaria. *XXI International Congress of the CBGA, Salzburg, Austria, Abstracts*.

Balkanska E., Georgiev S., Kounov A., Tagami T. & Sueoka S. 2021: Fission-track analysis using LA-ICP-MS: techniques and procedures adopted at the new low-temperature Thermochronology Laboratory in Bulgaria. *Comptes rendus de l'Academie bulgare des Sciences* 74, 102–109. https://doi.org/10.7546/CRABS.2021.01.13

Bergerat F., Vangelov D. & Dimov D. 2010: Brittle deformation, paleostress field reconstruction and tectonic evolution of the Eastern Balkanides (Bulgaria) during Mezozoic and Cenozoic times. In: Sosson M., Kaymakci N., Stephenson R.A., Bergerat F. & Starostenko V. (Eds.): Sedimentary Basin Tectonics from the Black Sea and Caucasus to the Arabian Platform. *Geological Society, London, Special Publications* 340, 77–111.

Boccaletti M., Manetti P., Peccerillo A. & Stanisheva-Vassileva G. 1978: Late Cretaceous high-potassium volcanism in Eastern Srednogorie, Bulgaria. *Geological Society of America Bulletin* 89, 439–447. https://doi.org/10.1130/0016-7606(1978)89<439:LCHVIE>2.0.CO;2

Bončev E. 1940: Über die Geologie des Bajlovo Teiles der Panagjuriste – Zone der Srednogorie unter Berücksichtigung der Tektonik dieser Zone. *Review of the Bulgarian Geological Society* 11, 205–238 (in Bulgarian).

Bončev E. 1970: On certain tectonic problems of the Srednogorie zone. *Review of the Bulgarian Geological Society* 31, 281–288 (in Bulgarian).

Bonev N., Spikings R. & Moritz R. 2020: $^{40}Ar/^{39}Ar$ age constraints for an early Alpine metamorphism of the Sakar unit, Sakar–Strandzha zone, Bulgaria. *Geological Magazine* 157, 1–7. https://doi.org/10.1017/S0016756820000953

Boyanov I., Zagorchev I. & Goranov A. 2003: Paleogene sediments (Mechit Formation) near Panagyurishte and Strelcha (Sredna gora Mts.). *Geologica Balcanica* 33, 15–22.

Burchfiel B.C. & Nakov R. 2015: The multiply deformed foreland foldthrust belt of the Balkan orogen, northern Bulgaria. *Geosphere* 11, 463–490. https://doi.org/10.1130/GES01020.1

Burchfiel B.C., Nakov R., Dumurdžanov N. et al. 2008: Evolution and dynamics of the Cenozoic tectonics of the South Balkan extensional system. *Geosphere* 4, 919–938. https://doi.org/10.1130/GES00169.1

Caracciolo L., Orlando A., Critelli S., Kolios N., Manetti P. & Marchev P. 2015: The tertiary Thrace basins of SE Bulgaria and NE Greece: a review of petrological and mineralogical data of sedimentary sequences. *Acta Vulcanologica*, 25, 21–41.

Carlson W., Donelick R. & Ketcham R. 1999: Variability of apatite fission-track annealing kinetics: I. Experimental results. *American Mineralogist* 84, 1213–1223. https://doi.org/10.2138/am-1999-0901

Carrigan C.W., Mukasa S.W., Haydoutov I. & Kolcheva K. 2005: Age of Variscan magmatism from the Balkan sector of the orogen, central Bulgaria. *Lithos* 82, 125–147. https://doi.org/10.1016/j.lithos.2004.12.010

Carrigan C.W., Mukasa S.W., Haydoutov I. & Kolcheva K. 2006: Neoproterozoic magmatism and Carboniferous high-grade metamorphism in the Sredna Gora Zone, Bulgaria: An extension of the Gondwana-derived Avalonian-Cadomian belt? *Precambrian Research* 147, 404–416. https://doi.org/10.1016/j.precamres.2006.01.026

Cavazza W., Caracciolo L., Critelli S., d'Atri A. & Zuffa G.G. 2013: Petrostratigraphic evolution of the Thrace basin (Bulgaria, Greece, Turkey) within the context of Eocene–Oligocene post-collisional evolution of the Vardar–Izmir–Ankara suture zone. *Geodinamica Acta* 26, 12–26. https://doi.org 10.1080/09853111.2013.858943

Corrigan J.D. 1993: Apatite fission-track analysis of Oligocene strata in South Texas, USA; testing annealing models. *Chemical Geology* 104, 227–249. https://doi.org/10.1016/0009-2541(93)90153-A

Dabovski Ch., Zagorchev I., Ruseva M. & Chunev D. 1966: The Paleozoic granitoids of the Sashtinska Sredna Gora. *Annuaire de la Direction Generale de Géologie* 16, 57–96 (in Bulgarian).

Dabovski H., Sinnyovsky D., Vasilev E. & Dimitrova E. 2009: Upper Cretaceous geology – Stratigraphy. In: Zagorchev I., Dabovski C. & Nikolov T. (Eds.): Geology of Bulgaria. Volume II. Mesozoic geology. *"Prof. Marin Drinov" Academic Publishing House,* Sofia, 15–37 (in Bulgarian).

Dimitrova E., Nachev I. & Slavov S. 1984: Upper Cretaceous stratigraphy of the Panagyurishte area. *Bulletin of the Geological Institute, Bulgarian Academy of Sciences, Series Paleontology, Stratigraphy, Lithology* 19, 65–83 (in Bulgarian).

Ehlers T., Chaudhri T., Kumar S., Fuller C., Willett S., Ketcham R., Brandon M., Belton D., Kohn B., Gleadow A., Dunai T. & Fu F. 2005: Computational tools for low-temperature thermochronometer interpretation. *Reviews in Mineralogy and Geochemistry* 58, 589–622. https://doi.org/10.2138/rmg.2005.58.22

Fitzgerald P.G. & Malusà M.G. 2019: Concept of the exhumed partial annealing (retention) zone and age-elevation profiles in thermochronology. In: Malusà M.G. & Fitzgerald P.G. (Eds.): Fission-track thermochronology and its application to Geology. *Springer International Publishing*, 165–190.

Gaggero L., Buzzi L., Haydoutov I. & Cortesogno L. 2009: Eclogite relics in the Variscan orogenic belt of Bulgaria (SE Europe). *International Journal of Earth Sciences* 98, 1853–1877. https://doi.org/10.1007/s00531-008-0352-x

Gallagher K. 2012: Transdimensional inverse thermal history modeling for quantitative thermochronology. *Journal of Geophysical Research: Solid Earth* 117, B02408. https://doi.org/10.1029/2011JB008825

Gallhofer D., von Quadt A., Peytcheva I., Schmid S. & Heinrich A.C. 2015: Tectonic, magmatic and metallogenic evolution of the Late Cretaceous Arc in the Carpathian-Balkan orogen. *Tectonics* 34, 1813–1836. https://doi.org/10.1002/2015TC003834

Gerdjikov I. & Georgiev N. 2005: Spectacular fabric but little displacement: Early Alpine shear zones from Zlatishka Stara Planina, Central Balkanides. *Proceedings of Jubilee International conference "Geosciences 2005". Bulgarian Geological Society,* Sofia, 35–38.

Gerdjikov I. & Georgiev N. 2006: The Maritsa fault zone – a strike-slip zone along the northern margin of the Rhodopes. *Journal of Mining and Geological Sciences* 49, 33–39.

Gerdjikov I., Georgiev N., Dimov D. & Lazarova A. 2007: The different faces of supposedly single thrust: a reevaluation of the Vezhen thrust, Central Balkanides. *Proceeding of National conference "Geosciences 2008". Bulgarian Geological Society,* Sofia, 24–26.

Gerdjikov I., Ruffet G., Lazarova A., Vangelov D., Balkanska E. & Bonev K. 2010: $^{40}Ar/^{39}Ar$ geochronological constrains of a Variscan transpression in Central Stara Planina Mountain. *Proceedings of the National Conference "Geosciences", Bulgarian Geological Society*, 109–110.

Gerdjikov I., Radulov A. & Metodiev L. 2015: Cretaceous–Tertiary deformations along a part of the Maritsa fault system between Pazardzhik and Sofia. *Proceedings of the National Conference "Geosciences", Bulgarian Geological Society*, 89–90.

Gerdjikov I., Vangelov D. & Kounov A. 2019: Main fault zones controlling the late Alpine structure in the area east of Sofia (Srednogorie Zone, Western Bulgaria). *Journal of Mining and Geological Sciences* 62, 71–76.

Gerdjikov I., Dinev Y. & Vangelov D. 2020: Structural geology of the central part of Kamenitsa–Rakovishka fault zone. *Journal of Mining and Geological Sciences* 63, 214–219.

Gleadow A.J.W. & Duddy I.R. 1981: A natural long-term track annealing experiment for apatite. *Nuclear Tracks* 5, 169–174. https://doi.org/10.1016/0191-278X(81)90039-1

Gleadow A., Harrison M., Kohn B., Lugo-Zazueta R. & Phillips D. 2015: The Fish Canyon Tuff: A new look at an old low-temperature thermochronology standard. *Earth and Planetary Science Letters* 424, 95–108. http://doi.org/10.1016/j.epsl.2015.05.003

Green P.F. & Duddy I.R. 1989: Some comments on paleotemperature estimation from apatite fission track analysis. *Journal of Petro-*

leum Geology 12, 111–114. https://doi.org/10.1111/j.1747-5457.1989.tb00224.x

Gunnell Y., Calvet M., Meyer B., Pinna-Jamme R., Bour I., Gautheron C., Carter A. & Dimitrov D. 2017: Cenozoic landforms and post-orogenic landscape evolution of the Balkanide orogen: Evidence for alternatives to the tectonic denudation narrative in southern Bulgaria. *Geomorphology* 276, 203–221. https://doi.org/10.1016/j.geomorph.2016.10.015

Handler R., Neubauer F., Velichkova S. & Ivanov Z. 2004: $^{40}Ar/^{39}Ar$ age constraints on the timing of magmatism in the Panagyurishte region, Bulgaria. *Schweizerische Mineralogische und Petrographische Mitteilungen* 84, 119–132. http://doi.org/10.5169/seals-63742

Harrison T.M., Duncan I. & McDougall I. 1985: Diffusion of ^{40}Ar in biotite – temperature, pressure and compositional effects. *Geochimica et Cosmochimica Acta* 49, 2461–2468. https://doi.org/10.1016/0016-7037(85)90246-7

Harrison M.T., Célérier J., Aikman A.B., Hermann J. & Heizler M.T. 2009: Diffusion of ^{40}Ar in muscovite. *Geochimica et Cosmochimica Acta* 73, 1039–1051. https://doi.org/10.1016/j.gca.2008.09.038

Hasebe N., Barbarand J., Jarvis K., Carter A. & Hurford A.J. 2004: Apatite fission-track chronometry using laser ablation ICP-MS. *Chemical Geology* 207, 135–45. https://doi.org/10.1016/j.chemgeo.2004.01.007

Hasebe N., Tamura A. & Arai S. 2013: Zeta equivalent fission-track dating using LA–ICP–MS and examples with simultaneous U–Pb dating, *Island Arc* 22, 280–291. https://doi.org/10.1111/iar.12040

Iliev K. & Katskov N. 1990: Geological Map of the Republic of Bulgaria in scale 1:100 000, Panagyurishte map sheet. *Committee of Geology,* Sofia.

Ivanov Ž. 1983: Apercu general sur l`evolution geologique des Balkanides. In: Ivanov Z. & Nikolov T. (Eds.): Guide to excursion. Sofia, 1–326.

Ivanov Ž. 2017: Tectonics of Bulgaria. *Sofia University Press*, Sofia, 1–331 (in Bulgarian).

Kamenov B., Yanev Y., Nedialkov R., Moritz R. Peytcheva I., von Quadt A., Stoykov S. & Zartova A. 2007: Petrology of Upper Cretaceous island-arc ore-magmatic centers from Central Srednogorie, Bulgaria: Magma evolution and paths. *Geochemistry, Mineralogy and Petrology* 45, 39–77.

Karagjuleva J., Kostadinov V. & Tzankov Tz. 1972: On the fault predestination of the Panagyuriste strip, to the east of the Topolnitsa River. *Comptes rendus de l'Academie bulgare des Sciences* 25, 1.

Karagjuleva J., Kostadinov V., Tzankov Tz. & Gočev P. 1974: Structure of the Panagjurište strip east of the Topolnica River. *Bulletin of the Geological Institute, Bulgarian Academy of Sciences, Series Geotectonics* 23, 231–301 (in Bulgarian).

Katskov N. & Iliev K. 1993: Explanatory note to the Geological Map of Bulgaria in scale 1:100 000, Panagjurishte map sheet. *Publ. "Geology and Geophysics"*, Sofia, 1–53 (in Bulgarian).

Ketcham R.A. 2005: Forward and inverse modeling of low-temperature thermochronometry data. *Reviews in Mineralogy and Geochemistry* 58, 275–314. https://doi.org/10.2138/rmg.2005.58.11

Ketcham R.A., Carter A., Donelick R.A., Barbarand J. & Hurford A.J. 2007: Improved modeling of fission-track annealing in apatite. *American Mineralogist* 92, 799–810. https://doi.org/10.2138/am.2007.2281

Kirchenbaur M., Pleuger J., Jahn-Awe S., Nagel T. J., Froitzheim N., Fonseca R. O. C. & Münker C. 2012. Timing of high-pressure metamorphic events in the Bulgarian Rhodopes from Lu-Hf garnet geochronology. *Contributions to Mineralogy and Petrology* 163, 897–921. https://doi.org/10.1007/s00410-011-0705-5

Koppers A.A.P. 2002: ArArCALC – software for Ar-40/Ar-39 age calculations. *Computers and Geosciences* 28, 605–619. https://doi.org/10.1016/S0098-3004(01)00095-4

Kounov A. & Gerdjikov I. 2020: The problems of the post-Cenomanian tectonic evolution of the central parts of the Sredna Gora Zone. The wrench tectonics – how real is real. *Geologica Balcanica* 49, 39–58.

Kounov A., Seward D., Bernoulli D. et al. 2004: Thermotectonic evolution of an extensional dome: the Cenozoic Osogovo–Lisets core complex (Kraishte zone, western Bulgaria). *International Journal of Earth Sciences* 93, 1008–1024. https://doi.org/10.1007/s00531-004-0435-2

Kounov A., Wüthrich E., Seward D., Burg J-P. & Stockli D. 2015: Low-temperature constraints on the Cenozoic thermal evolution of the Southern Rhodope Core Complex (Northern Greece). *International Journal of Earth Sciences* 104, 1337–1352. https://doi.org/10.1007/s00531-015-1158-2

Kounov A., Gerdjikov I., Vangelov D., Balkanska E., Lazarova A., Georgiev S., Blunt E. & Stockli D. 2018: First thermochronological constraints on the Cenozoic extension along the Balkan fold-thrust belt (Central Stara Planina Mountains, Bulgaria). *International Journal of Earth Sciences* 107, 1515–1538. https://doi.org/10.1007/s00531-017-1555-9

Kounov A., Seward D., Burg J.P., Stockli D. & Wüthrich E. 2020: Cenozoic thermal evolution of the Central Rhodope Metamorphic Complex (Southern Bulgaria). *International Journal of Earth Sciences* 109, 1589–1611. https://doi.org/10.1007/s00531-020-01862-4

Kuiper K.F., Deino A., Hilgen F.J., Krijgsman W., Renne P.R. & Wijbrans J.R. 2008: Synchronizing rock clocks of earth history. *Science* 320, 500–504. https://doi.org/10.1126/science.1154339

Lazarova A. & Gerdjikov I. 2008: Structures of sheared granitoids from the Zlatishka Stara Planina Mountain: indicators for the deformation at frictional-viscous transition. *Review of the Bulgarian Geological Society* 69, 7–20 (in Bulgarian).

Lazarova A., Naydenov K., Petrov N. & Grozdev V. 2015: Cambrian magmatism, Variscan high-grade metamorphism and imposed greenschist facies shearing in the Central Sredna Gora basement units (Bulgaria). *Geologica Carpathica* 66, 443–454. https://doi.org/10.1515/geoca-2015-0037

Lee J.Y., Marti K., Severinghaus J.P., Kawamura K., Yoo H.S., Lee J.B. & Kim J.S. 2006: A redetermination of the isotopic abundances of atmospheric Ar. *Geochimica Et Cosmochimica Acta* 70, 4507–4512.

Lo C.-H., Lee J.K.W. & Onstott T.C. 2000: Argon release mechanism of biotite in vacuo and the role of short-circuit diffusion and recoil. *Chemical Geology* 165, 135–166. https://doi.org/10.1016/S0009-2541(99)00167-9

Min K.W., Mundil R., Renne P.R. & Ludwig K.R. 2000: A test for systematic errors in Ar-40/Ar-39 geochronology through comparison with U/Pb analysis of a 1.1-Ga rhyolite. *Geochimica Et Cosmochimica Acta* 64, 73–98. https://doi.org/10.1016/S0016-7037(99)00204-5

Moev M. & Antonov M. 1978: Stratigraphy of the Upper Cretaceous in the eastern part of the Sturguel-Tchelopech strip. *Annual of the University of Mining and Geology, Faculty of Geology and Geophysics* 28, 7–30 (in Bulgarian).

Nachev I. & Nachev R. 2001: Alpine plate tectonics of Bulgaria. *Artik*, Sofia, 1–198 (in Bulgarian).

Naydenov K., Peytcheva I., von Quadt A., Sarov S., Kolcheva K. & Dimov D. 2013: The Maritsa strike-slip shear zone between Kostenets and Krichim towns, South Bulgaria – Structural, petrographic and isotope geochronology study. *Tectonophysics* 595–596, 69–89. https://doi.org/10.1016/j.tecto.2012.08.005

Nedialkov R., Zartova A. & Moritz R. 2007: Magmatic rocks and evolution of the Late Cretaceous magmatism in the region of

the Asarel porphyry copper deposit, Central Srednogorie, Bulgaria. *Review of the Bulgarian Geological Society* 68, 57–76.

Pavlishina P. 2002: Danian Normapolles from the conglomeratic formation near Panagyurishte and Strelcha (Sredna Gora Mountins, Bulgaria. *Geologica Balcanica* 32, 209–213.

Peytcheva I. & von Quadt A. 2004: The Palaeozoic protoliths of Central Srednogorie, Bulgaria: records in zircons from basement rocks and Cretaceous magmatites. *5th International Symposium on Eastern Mediterranean Geology, Thessaloniki, Greece, Conf. Vol.*, Extended abstract, T11-9.

Peytcheva I., von Quadt A., Kouzmanov K. & Bogdanov K. 2003: Elshitsa and Vlaykov Vruh epithermal and porphyry Cu (–Au) deposits of Central Srednogorie, Bulgaria: source and timing of magmatism and mineralisation. In: Eliopoulos D.G. et al. (Eds.): Mineral Exploration and Sustainable Development. *Millpress*, Rotterdam, 371–373.

Peytcheva I., von Quadt A., Georgiev N., Ivanov Z., Heinrich C. & Frank M. 2008: Combining trace-element compositions, U–Pb geochronology and Hf isotopes in zircons to unravel complex calcalkaline magma chambers as inferred by mixed gabbros and granodiorites in the Upper Cretaceous Srednogorie zone (Bulgaria). *Lithos* 104, 405–427. https://doi.org/10.1016/j.lithos.2008.01.004

Peytcheva I., von Quadt A.; Neubeaur F. Frank M., Nedialkov R., Heinrich C.A. & Strashimirov St. 2009: U–Pb dating, Hf-isotope characteristics and trace-REE-patterns of zircons from Medet porphyry copper deposit, Bulgaria: implications for timing, duration and sources of ore-bearing magmatism. *Mineralogy and Petrology* 96, 19–41. https://doi.org/10.1007/s00710-009-0042-9

Popov P., Berza T., Grubic A. & Ioane D. 2002a: Late Cretaceous Apuseni–Banat–Timok–Srednogorie (ABTS) magmatic and metallogenic belt in the Carpathian-Balkan orogeny. *Geologica Balcanica* 32, 145–163.

Popov P., Radichev R. & Dimovski S. 2002b: Geology and evolution of the Elatsite–Chelopech porphyry-copper-massive sulfide ore field (in Bulgarian). *Annual book of the High Institute of Mining and Geology* 43/44, 31–44.

Popov K., Velichkov D. & Popov P. 2015: The post-collisional Upper Thracian Rift System (Bulgaria) and the formed exogenous uranium deposits, Part 1 – Lithostratigraphy and tectonic. *Review of the Bulgarian Geological Society* 76, 35–49.

Rahn M. & Seward D. 2000: How many track lengths do we need? *On Track* 10, 12–15.

Rieser B.A., Neubauer F., Handler R., Velichkova S. & Ivanov Z. 2008: New $^{40}Ar/^{39}Ar$ age constraints on the timing of magmatic events in the Panagyurishte region, Bulgaria. *Swiss Journal of Geosciences* 101, 107–123. https://doi.org/10.1007/s00015-007-1243-z

Sapoundjieva V. & Dragomanov L. 1991: Reference borehole in the Paleogene at Opálčenec village, Plovdiv area. *Review of the Bulgarian Geological Society* 52, 42–49 (in Bulgarian).

Schmid S.M., Bernoulli D., Fügenschuh B., Matenco L., Schefer S., Schuster R., Tichler M. & Ustaszewski K. 2008: The Alpine–Carpathian–Dinaridic orogenic system: correlation and evolution of tectonic units. *Swiss Journal of Geosciences* 101, 139–183. https://doi.org/10.1007/s00015-008-1247-3

Shi W., Wang F., Wu L., Yang L., Wang Y. & Shi G. 2020: Geologically meaningful $^{40}Ar/^{39}Ar$ ages of altered biotite from a polyphase deformed shear zone obtained by *in Vacuo* step-heating method: a case study of the Waziyü detachment fault, Northeast China. *Minerals* 10, 648. https://doi.org/10.3390/min10080648

Sinnyovsky D. 2004: Nannofossil subdivision and stratigraphic range of the Emine Flysch Formation in East Balkan, East Bulgaria. *Journal of Mining and Geological Sciences* 47, 131–137.

Stampfli G. M. & Hochard C. 2009: Plate tectonics of the Alpine realm. In: Murphy J. B., Keppie J. D. & Hynes A. J. (Eds.): Ancient Orogens and Modern Analogues. *Geological Society, London, Special Publications* 327, 89–111. https://doi.org/10.1144/SP327.6

Stanisheva-Vassileva G. 1980: The Upper Cretaceous magmatism in Srednogorie zone, Bulgaria: a classification attempt and some implications. *Geologica Balcanica* 10, 15–36.

Strashimirov S., Petrunov R. & Kanazirski M. 2002: Porphyry-copper mineralisation in the central Srednogorie zone, Bulgaria. *Mineralium Deposita* 37, 587–598. https://doi.org/10.1007/s00126-002-0275-6

Stübner K., Drost K., Schoenberg R., Böhme M., Starke J. & Ehlers T.A. 2016: Asynchronous timing of extension and basin formation in the South Rhodope core complex, SW Bulgaria, and northern Greece. *Tectonics* 35, 136–159. https://doi.org/10.1002/2015TC004044

Szopa K., Salacińska A., Gumsley A., Chew D., Petrov P., Gaweda A., Zagorska A., Deput E. Gospodinov N. & Banasik K. 2020: Two-stage Late Jurassic to Early Cretaceous hydrothermal activity in the Sakar Unit of Southeastern Bulgaria. *Minerals* 10, 266. https://doi.org/10.3390/min10030266

Tagami T. 2005: Zircon fission-track thermochronology and Applications to fault studies. *Reviews in Mineralogy and Geochemistry* 58, 95–122. https://doi.org/10.2138/rmg.2005.58.4

Tagami T. & Dumitru T.A. 1996: Provenance and history of the Franciscan accretionary complex: Constraints from zircon fission track thermochronology. *Journal of Geophysical Research* 101, 8345–8255. https://doi.org/10.1029/96JB00407

Tagami T., Uto K., Matsuda T., Hasebe N. & Matsumoto A. 1995: K-Ar biotite and fission-track zircon ages of the Nisatai Dacite, Iwate Prefecture, Japan: A candidate for Tertiary age standard. *Geochemical Journal* 29, 207–211.

Tagami T., Galbraith R.F., Yamada R. & Laslett G.M. 1998: Revised annealing kinetics of fission tracks in zircon and geological implications. In: van den Haute P. & de Corte F. (Eds.): Advances in Fission-Track Geochronology. *Solid Earth Sciences Library*, *Springer* 10, 99–112. https://doi.org/10.1007/978-94-015-9133-1_8

Vangelov D., Gerdjikov I., Kounov A. & Lazarova A. 2013: The Balkan Fold-Thrust Belt: an overview of the main features. *Geologica Balcanica* 42, 29–47.

Vangelov D., Gerdjikov I., Dochev D., Dotseva Z., Velev S., Dinev Y., Trayanova D. & Dancheva J. 2019: Upper Cretaceous lithostratigraphy of the Panagyurishte strip (Central Bulgaria) – part of the Late Cretaceous Apuseni–Banat–Timok–Srednogorie magmatic belt. *Geologica Balcanica* 48, 11–33.

Velichkova S., Handler R., Neubauer F. & Ivanov Z. 2004: Variscan to Alpine tectonothermal evolution of the Central Srednogorie unit, Bulgaria: constraints from $^{40}Ar/^{39}Ar$ analysis. *Schweizerische Mineralogische und Petrographische Mitteilungen* 84, 133–151. https://doi.org/10.5169/seals-63743

Vermeesch P. 2018: IsoplotR: A free and open toolbox for geochronology. *Geoscience Frontiers* 9, 1479–1493. https://doi.org/10.1016/j.gsf.2018.04.001

Vermeesch P. & Tian Y. 2014: Thermal hostory modelling: HeFTy vs. QTQt. *Earth-Science Reviews* 139, 279–290. https://doi.org/10.1016/j.earscirev.2014.09.010

von Quadt A., Peytcheva I., Frank M., Nedyalkov R., Kamenov B. & Heinrich C. 2004: Subduction related rocks in Medet Cu-porphyry deposit: Sources and magma evolution. *Goldschmidt Conference Abstracts*, 626.

von Quadt A., Moritz R., Peytcheva I. & Heinrich C.A. 2005: Geochronology and geodynamics of Late Cretaceous magmatism and Cu-Au mineralization in the Panagyurishte region of the Apuseni–Banat–Timok–Srednogorie belt, Bulgaria.

Ore Geology Reviews 27, 95–126. https://doi.org/10.1016/j.oregeorev.2005.07.024

Wijbrans J.R., Pringle M.S., Koppers A.A.P. & Scheveers R. 1995: Argon geochronology of small samples using the VULKAAN laserprobe. *Proceedings of the Koninklijke Nederlandse Akademie Van Wetenschappen-Biological Chemical Geological Physical and Medical Sciences* 98, 185–218.

Yamada R., Tagami T., Nishimura S. & Ito H. 1995: Annealing kinetics of fission tracks in zircon: an experimental study. *Chemical Geology* 122, 246–248. https://doi.org/10.1016/0009-2541(95)00006-8

Yamada R., Murakami M. & Tagami T. 2007: Statistical modelling of annealing kinetics of fission tracks in zircon; Reassessment of laboratory experiments. *Chemical geology* 236, 75–91. https://doi.org/10.1016/j.chemgeo.2006.09.002

Zagorchev I. 2008: Amphibolite-facies metamorphic complexes in Bulgaria and Precambrian geodynamics: controversies and "state of the art". *Geologica Balcanica* 37, 33–46.

Zagorchev I & Budurov K. 2009: Triassic geology. In: Zagorchev I., Dabovski C. & Nikolov T. (Eds.): Geology of Bulgaria. Volume II. Mesozoic geology. *"Prof. Marin Drinov" Academic Publishing House,* Sofia, 39–130 (in Bulgarian).

Zagorchev I., Dabovsky Ch. & Tchunev D. 1973: Tectonics of western part of the Sredna Gora metamorphic block (Sashtinska Sredna Gora). *Review of the Bulgarian Geological Society* 37, 1–10 (in Bulgarian).

Zagorchev I., Pavlishina P., Cernjavska S., Boyanov I. & Goranov A. 2001: First data on a Danian age of the conglomeratic formation near Panagyurishte and Strelcha (Sredna-Gora Mountains). *Comptes rendus de l'Académie bulgare des Sciences* 54, 53–56.

Zagorchev I., Dabovski C. & Nikolov T. (Eds.). 2009: Geology of Bulgaria. Volume II. Mesozoic geology. *"Prof. Marin Drinov" Academic Publishing House,* Sofia, 1–765 (in Bulgarian).

Zimmerman A., Stein H., Hannah J., Koželj D., Bogdanov K. & Berza T. 2008: Tectonic configuration of the Apuseni–Banat–Timok–Srednogorie belt, Balkans-South Carpathians, constrained by high precision Re–Os molybdenite ages. *Mineralium Deposita* 43, 1–21. https://doi.org/10.1007/s00126-007-0149-z

Appendix

Sample	Mineral	Grains	Ns	ps ($10^6 cm^{-2}$)	238 U (ppm)	T pooled ±1 σ (Ma)	P(χ2) %	Reference
Fish Canyon Tuff 1	apatite	17	200	0.2	14.8	30.6 ± 2.8	99.93	Gleadow et al. (2015)
Fish Canyon Tuff 2	apatite	16	231	0.2	15	27.4 ± 2.0	24.85	Gleadow et al. (2016)
Fish Canyon Tuff	zircon	19	547	5.8	403.9	26.7 ± 1.3	0	Gleadow et al. (2017)
Nisatai Dacite	zircon	21	378	3.3	264.1	23.3 ± 1.3	6.81	Tagami et al. (1995)

Electronic supplementary material is available online:
Supplementary Table S1 at http://geologicacarpathica.com/data/files/supplements/GC-73-1-Balkanska_Table_S1.xlsx